

# The QCD Phase Boundary from Quark-Gluon Dynamics

Jens Braun

*TRIUMF, 4004 Wesbrook Mall, Vancouver, BC V6T 2A3, Canada*

(Dated: November 7, 2018)

We study one-flavor QCD at finite temperature and chemical potential using the functional renormalization group. We discuss the chiral phase transition in QCD and its order with its underlying mechanism in terms of quarks and gluons and analyze the dependence of the phase transition temperature on small quark chemical potentials. Our result for the curvature of the phase boundary at small quark chemical potential relies on only a single input parameter, the value of the strong coupling at the  $Z$  mass scale.

PACS numbers: 12.38.Aw, 64.60.ae

## I. INTRODUCTION

The phase boundary of Quantum Chromodynamics (QCD) is currently a very active frontier both theoretically and experimentally. For fixed small quark chemical potentials, the ground-state of QCD changes with increasing temperature from a hadronic phase with dynamically broken chiral symmetry to a deconfined quark-gluon plasma phase with an effectively restored chiral symmetry. Even though the phase transition temperatures are not directly observable in heavy-ion collision experiments at BNL and CERN, a lower bound can be extracted from the experimental data [1]. These so-called chemical freeze-out temperatures can then be compared to theoretical predictions for the chiral and deconfinement phase-transition temperature. Since QCD is a strongly-interacting theory and long-range fluctuations need to be captured in order to study phase transitions, non-perturbative approaches are indispensable for a study of the QCD phase boundary.

On the theoretical side, various approaches are available for studies of the QCD phase boundary, e. g. lattice QCD simulations or functional methods. Each of these approaches comes with advantages and disadvantages. Lattice QCD simulations are certainly the most powerful tool for a study of full QCD. However, the implementation of chiral fermions

continues to be a non-trivial task. At finite chemical potential, the spectrum of the Dirac operator becomes complex, making direct lattice simulations even more difficult. In the past decade, however, several methods have been developed to circumvent the problems arising at finite chemical potential, such as studies of QCD at imaginary chemical potential [2, 3, 4, 5], Taylor expansions of the path integral or reweighting techniques [6, 7, 8, 9, 10], see e. g. Refs. [11, 12] for short overviews.

Functional approaches to QCD, such as mean-field studies, Dyson-Schwinger Equations or Renormalization Group approaches, do not have problems arising from a discretized action or a complex-valued spectrum of the Dirac operator. However, a study of full QCD is not possible and a truncation of the QCD action functional is unavoidable. Therefore Lattice QCD simulations and continuum approaches should be considered as complementary approaches for studies of the QCD phase diagram.

Dynamical chiral symmetry breaking has been studied by applying effective low-energy models such as the Nambu-Jona-Lasinio (NJL) model [13]. The application of these models is built on the assumption that QCD falls into a certain universality class, namely  $O(4)$ . Whether this assumption is justified or not is currently under investigation by Lattice QCD simulations as well as functional RG methods [14, 15, 16, 17, 18].

Although NJL-type models already allow to study dynamical chiral symmetry breaking at finite temperature and quark chemical potential, they do not contain gluonic degrees of freedom and they are not confining. Moreover, an ultraviolet (UV) cutoff has to be introduced in the theory. This makes the connection of these models to high-momentum scales and temperatures difficult. The dependence on the UV cutoff implies a parameter dependence of the model. The strategy for employing these models is usually as follows: First, one uses a set of parameters and the UV cutoff to fit the values of low-energy observables at zero temperature and zero chemical potential, e. g. to the pion mass and to the pion decay constant. Second, one computes the phase boundary of QCD while keeping the parameters and the UV cutoff fixed. A shortcoming of these models is apparent: The set of parameters used to fit a given set of low-energy observables is not unique. Even worse, two sets of parameters, which both give the same results for the low-energy observables, do not necessarily lead to the same results for the chiral phase boundary and the location of the critical endpoint is not necessarily the same [19].

In the past few years, quite some progress has been made in connecting the low-energy

regime described by quark-meson dynamics with the dynamics at high temperatures, see e. g. Refs. [20, 21, 22, 23, 24, 25, 26, 27]. Such improved models for a description of the QCD dynamics at finite temperature and density are mostly based on the inclusion of a Polyakov-Loop potential extracted from lattice QCD results. By this means, the treatment of the gauge-field dynamics has been outsourced while the less problematic quark-meson dynamics are treated self-consistently within the framework. Although all of these approaches provide us with a better understanding of the thermodynamics of QCD at low and high temperatures, they cannot get rid of the parameter dependence of the results. In addition, the back-reaction of the quark-dynamics on the gauge-field dynamics in terms of the Polyakov-Loop has not yet been fully taken into account. For a quantitative description of the QCD phase boundary, however, not only the gauge-field dynamics need to be taken into account: The fluctuations of the Goldstone modes and the radial mode beyond the mean-field approximation also play an important role at the phase boundary, in particular with respect to a better description of the susceptibilities in QCD with physical pion masses.

In this paper, we discuss a functional Renormalization Group (RG) approach to the QCD phase boundary. The chiral phase boundary of the quark-meson model (bosonized NJL model) with two degenerate quark flavors has been studied in the local potential approximation using a functional RG approach in Ref. [28]. The advantage of the approach presented in this work is that it allows not only for dynamical chiral symmetry breaking triggered by gluodynamics but also provides access to the infrared domain of QCD dominated by pions. Our approach is based on ground-breaking work done by H. Gies and C. Wetterich, see Refs. [29, 30]. There it has been shown for vanishing temperature and quark chemical potential that both the regime dominated by Goldstone modes and the perturbative QCD regime dominated by quark-gluon dynamics can be conveniently linked without fine-tuning using the functional RG. In Refs. [31, 32], the chiral phase boundary in the plane of temperature and number of quark flavors has been computed by studying quark-gluon dynamics using the functional RG. The strategy of the latter papers was to determine for which temperatures and number of quark flavors QCD remains in the chirally symmetric regime and thereby implicitly extracting the phase transition temperatures. In contrast, this paper aims to set the stage for studies of the QCD phase boundary with two and three quark flavors including the possibility to study the low-temperature regime and the order of the chiral phase transition. To this end, we use the approach discussed in Refs. [29, 30] and combine

it with the findings of Refs. [31, 32]: Our strategy is to follow the RG flow starting at high momentum scales ( $p \sim M_Z$ ) down to the deep infrared regime which is dominated by the dynamics of Goldstone modes. This allows us to get rid of the unwanted ambiguity in the parameter-space as it is present in NJL-type models. Our results for the phase boundary will depend on only a single input parameter, namely the value of the strong coupling  $\alpha_s$  at the initial RG scale. By this means, the scale is set unambiguously in our calculations and the values of all dimensionful quantities, such as the constituent quark mass or the chiral phase transition temperature, are eventually determined by the choice of the initial value of the strong coupling only.

The paper is organized as follows: In Sect. II, we give a discussion of the technical details of our functional RG approach for a study of the QCD phase boundary. Our results for the chiral phase boundary at small quark chemical potentials for QCD with one quark flavor including a comparison to lattice QCD results are then discussed in Sect. III. We also discuss the possibility of merging our work with recent studies of the deconfinement phase-transition in pure Yang-Mills theory using functional RG methods [33, 34]. Our concluding remarks, including a discussion of future extensions, are presented in Sect. IV.

## II. RG FLOW OF THE EFFECTIVE ACTION

Throughout this paper we work in  $d = 4$  dimensional Euclidean space and employ the following ansatz for the effective action for our study of the phase diagram of 1-flavor QCD:

$$\Gamma = \int d^4x \left\{ Z_\psi \bar{\psi} (i \not{D}[A] + i \gamma_0 \mu) \psi + \frac{\bar{\lambda}_\sigma}{2} [(\bar{\psi} \psi)^2 - (\bar{\psi} \gamma_5 \psi)^2] + \frac{1}{2} Z_\phi (\partial_\mu \Phi)^2 + U(\Phi^2) \right. \\ \left. + \frac{\bar{h}}{\sqrt{2}} (\bar{\psi} (\vec{\tau} \cdot \Phi) \psi) + \frac{Z_F}{4} F_{\mu\nu}^a F_{\mu\nu}^a + \frac{1}{2\xi} (D_\mu [\bar{A}] a_\mu^a)^2 \right\} + \Gamma_{\text{gauge}}, \quad (1)$$

where  $D_\mu^{ij} = \partial_\mu \delta^{ij} - i g T_a^{ij} A_\mu^a$ , with  $T_a$  being the hermitean gauge-group generators of the gauge group in the fundamental representation. We have introduced the shorthand  $(\bar{\psi} \psi) = \bar{\psi}^i \psi_i$  for the color indices. In the gauge sector we have included a background gauge fixing term,  $\xi$  being the gauge-fixing parameter. We split up the gauge field into a background field  $\bar{A}_\mu$  and a fluctuation field  $a_\mu$ , i. e.  $A_\mu = \bar{A}_\mu + a_\mu$ . The term  $\Gamma_{\text{gauge}}$  contains the ghost sector and possible higher-order gluonic operators. We shall discuss this part of the truncation in more detail in Sec. II F. The scalar fields are combined in the  $O(2)$  vector  $\Phi^T = (\Phi_1, \Phi_2)$  and we have used  $\vec{\tau} = (\gamma_5, i \cdot \mathbf{1}_d)$  in order to define the Yukawa interaction. The initial conditions

for the various couplings in Eq. (1) at the ultraviolet (UV) scale  $\Lambda$  are chosen such that the initial effective action is given by the (classical) QCD action functional:

$$\Gamma_{k=\Lambda} = \int d^4x \left\{ \frac{1}{4} F_{\mu\nu}^a F_{\mu\nu}^a + \bar{\psi} i \not{D} \psi \right\}, \quad (2)$$

see also the discussion in Sec. III A. While the inclusion of higher gluonic operators is discussed in Sec. II F, the quark-meson part of our truncation is built around the standard mean-field ansatz of the effective action (large  $N_c$  ansatz; standard NJL model ansatz), i. e. ( $Z_\phi(k=\Lambda) = 0, \partial_t Z_\phi = 0; Z_\psi(k=\Lambda) = 1, \partial_t Z_\psi = 0$ ), which has been used extensively for studies of the QCD phase diagram, see e. g. Refs. [35, 36]. Such an ansatz underlies also most of the recent (P)NJL studies of hot and dense QCD, see e. g. Refs. [22, 24, 25, 26, 27].

In the present paper, we are aiming at a dynamical connection of the high- and low-momentum regime of QCD. Therefore we have to go beyond the zeroth-order ansatz (standard NJL-model ansatz) for the effective action. In the following we systematically extend this zeroth-order ansatz in two directions, namely in derivatives and  $n$ -point functions  $\Gamma^{(n)}$  where  $n$  defines the number of legs. In order to study spontaneous symmetry breaking indicated by a non-trivial minimum of the order-parameter potential  $U(\Phi^2)$  in Eq. (1), we expand the potential in powers of  $\Phi^2$  resulting in RG flow equations for the mesonic  $n$ -point functions, see Sec. II A for details. The quality of such a systematic expansion of the effective potential  $U(\Phi^2)$  has been studied quantitatively in Refs. [37, 38] and is well under control. On the other hand, we perform a derivative expansion which renders the  $n$ -point functions momentum-dependent. The latter is indispensable for a connection of the high- and low-momentum regime of QCD.

Next to the zeroth-order approximation one needs to include kinetic terms for the meson fields in the truncation. The minimal truncation which allows for an inclusion of meson loops is given by the so-called Local Potential Approximation (LPA), i. e. ( $Z_\phi(k=\Lambda) = 1, \partial_t Z_\phi = 0; Z_\psi(k=\Lambda) = 1, \partial_t Z_\psi = 0$ ). This truncation has been used, e. g., in Refs. [23, 39] for a study of the quark-meson model at finite temperature and density. It indeed turns out that the LPA represents already a major improvement with respect to the quality of the critical exponents; the quality of critical exponents can be considered as a measure of how good the dynamics at the phase transition are captured. In the present paper, we go also beyond this approximation and allow for a running of the wave-function renormalizations of

the quark and meson fields<sup>1</sup>, i. e. ( $Z_\phi(k=\Lambda) \rightarrow 0, \partial_t Z_\phi \neq 0; Z_\psi(k=\Lambda) = 1, \partial_t Z_\psi \neq 0$ ). Such a truncation renders the involved vertices momentum-dependent and improves the quality of the results as it can be read off from, e. g., the quality of the critical exponents<sup>2</sup>, see e. g. Refs. [37, 41, 42]. Aside from an extension of a given truncation with higher-order operators, an error estimate for a given truncation can be obtained by a variation of the regulator. By this means it was found in Ref. [43] that the present truncation (1) gives remarkably robust results when applied to a study of chiral symmetry breaking at vanishing temperature and chemical potential. Although we have not performed such a variation of the regulator in the present work, it is likely that the findings in Ref. [43] hold also in the present context of chiral symmetry breaking at finite temperature. This is due to the fact that chiral symmetry breaking sets in on scales  $T/k \lesssim 0.5$  as we shall see below.

We would like to point out that our truncation (1) is redundant since the four-fermion coupling  $\bar{\lambda}_\sigma$  is related to the scalar potential  $U(\Phi^2)$  and the Yukawa coupling  $\bar{h}$  via a Hubbard-Stratonovich transformation. However, this redundancy can be completely lifted by applying "re-bosonization" techniques [29, 30, 44] which we will use here. This allows us to conveniently bridge the gap between quark and gluon degrees of freedom in the UV and mesonic degrees of freedom in the infrared (IR) regime. Moreover, re-bosonization techniques allow us to conveniently include momentum-dependent fermionic  $n$ -point functions (four-fermion interactions, six-fermion interactions, ...) up to arbitrary order in the RG flow<sup>3</sup>. In this paper, we work along the lines of Ref. [30] and give only a brief discussion of the "re-bosonization"-procedure in Sec. II E.

The effective action (1) has a global  $U_A(1)$  symmetry. The breaking of this global symmetry is associated with topologically non-trivial gauge configurations. For the moment, we do not include terms that break this global symmetry, but we discuss the effect of such terms on our results in Sec. III. In one-flavor QCD, these gauge configurations play a very

---

<sup>1</sup> We would like to remark that a truncation with ( $Z_\phi(k=\Lambda) \rightarrow 0, \partial_t Z_\phi \neq 0; Z_\psi(k=\Lambda) = 1, \partial_t Z_\psi = 0$ ) represents the lowest order in the derivative expansion which allows for a dynamical connection of the high- and low-momentum regime of QCD, see discussion in Sec. II E and Refs. [29, 30].

<sup>2</sup> The derivative expansion can be continued systematically by, e. g. including terms of the form  $Y_k(\Phi \partial_\mu \Phi)^2$  in our truncation, see e. g. Ref. [40].

<sup>3</sup> Note that maximal  $n$  is related to the maximal order in our expansion of the order-parameter potential in  $\Phi^2$  ( $\Phi \sim \bar{\psi}\psi$ ) by means of the continuously performed Hubbard-Stratonovich transformations in the RG flow.

exposed role since they induce masslike fermion interactions which break the  $U_A(1)$  symmetry [45, 46, 47, 48]. The impact of gauge-field configurations with non-trivial topology on the nature of the chiral phase transition of 2-flavor QCD is not yet conclusively settled. In general, it is expected that such gauge-field configurations become less important with increasing number of quark flavors [49]. In this respect, we expect that dropping  $U_A(1)$  violating terms in our ansatz for the effective action of 1-flavor QCD makes the phase structure more closely comparable to QCD with more than one quark flavor.

For our derivation of the RG flow equations of the couplings, we employ the Wetterich equation [50]:

$$\partial_t \Gamma_k[\chi] = \frac{1}{2} \text{STr} \left\{ \left[ \Gamma_k^{(1,1)}[\chi] + R_k \right]^{-1} \cdot (\partial_t R_k) \right\} \quad \text{with} \quad \Gamma_k^{(1,1)}[\chi] = \frac{\overrightarrow{\delta}}{\delta \chi^T} \Gamma_k[\chi] \frac{\overleftarrow{\delta}}{\delta \chi}, \quad (3)$$

where  $t = \ln k/\Lambda$  and  $\Lambda$  is the UV cutoff. Here,  $\chi$  represents a vector in field space and is defined as

$$\chi^T \equiv \chi^T(-q) := (A_\mu^T(-q), \psi^T(-q), \bar{\psi}(q), \Phi_1(-q), \Phi_2(-q))$$

and

$$\chi \equiv \chi(q) := \begin{pmatrix} A_\mu(q) \\ \psi(q) \\ \bar{\psi}^T(-q) \\ \Phi_1(q) \\ \Phi_2(q) \end{pmatrix}.$$

Thus,  $\Gamma_k^{(1,1)}[\chi]$  is matrix-valued in field space and so is the regulator function  $R_k$ . In this work, we employ a  $3d$  optimized regulator function which is technically advantageous for studies at finite temperature [23, 51, 52]. The quality of such a  $3d$  regulator in the limit of vanishing temperature and chemical potential has been estimated by computing critical exponents of  $O(N)$  models [53] and comparing them to those obtained with an optimized regulator in  $4d$  space-time [54, 55]. Details on the regularization can be found in App. B. In the following we give the RG flow equations in a way which does not depend on the details of our  $3d$  regularization. Reviews on and introductions to the functional RG and its application to gauge theories can be found in Refs. [42, 44, 56, 57, 58].

Decomposing the inverse regularized propagator on the RHS of Eq. (3) into a field-independent and a field-dependent part,

$$\Gamma_k^{(1,1)}[\chi] + R_k = \mathcal{P}_k + \mathcal{F}_k, \quad (4)$$

we can expand the flow equation in powers of the fields:

$$\begin{aligned} \partial_t \Gamma_k &= \frac{1}{2} \text{STr} \left\{ \tilde{\partial}_t \ln(\mathcal{P}_k + \mathcal{F}_k) \right\} \\ &= \frac{1}{2} \text{STr} \left\{ \tilde{\partial}_t \left( \frac{1}{\mathcal{P}_k} \mathcal{F}_k \right) \right\} - \frac{1}{4} \text{STr} \left\{ \tilde{\partial}_t \left( \frac{1}{\mathcal{P}_k} \mathcal{F}_k \right)^2 \right\} + \frac{1}{6} \text{STr} \left\{ \tilde{\partial}_t \left( \frac{1}{\mathcal{P}_k} \mathcal{F}_k \right)^3 \right\} + \dots \end{aligned} \quad (5)$$

Here,  $\tilde{\partial}_t$  denotes a formal derivative acting only on the  $k$ -dependence of the regulator function  $R_k$ . The powers of  $\frac{1}{\mathcal{P}_k} \mathcal{F}_k$  can be computed by simple matrix multiplications. The flow equations for the various couplings can then be calculated by comparing the coefficients of the operators appearing on the RHS of Eq. (5) with the couplings specified in our truncation.

### A. RG flow of the effective potential

In this section we discuss the effective potential. The RG flow of the effective potential receives contributions from the scalar as well as the fermionic degrees of freedom:

$$U(\Phi) = U_B(\Phi) + U_F(\Phi). \quad (6)$$

It also depends implicitly and explicitly on the gauge degrees of freedom. The implicit dependence affects the running of the scalar couplings whereas the explicit dependence would result in additional terms in Eq. (6). Since we are not interested in thermodynamic quantities such as the pressure, but only in the order parameter, we can neglect these explicit contributions here. The contribution of the scalar fields to the effective potential is given by

$$\begin{aligned} U_B(\Phi) &= \frac{1}{2} T \sum_{n=-\infty}^{\infty} \int \frac{d^3 p}{(2\pi)^3} \bar{p}^2 (\partial_t r_{B,k}) \left\{ Z_{\sigma}^{\perp}(\omega_n, \{p_i\}) P_B(\bar{M}_{\sigma}(\Phi)) \right. \\ &\quad \left. + Z_{\pi}^{\perp}(\omega_n, \{p_i\}) P_B(\bar{M}_{\pi}(\Phi)) \right\}, \end{aligned} \quad (7)$$

where  $T$  defines the temperature and  $\omega_n = 2\pi nT$  denotes the bosonic Matsubara frequencies. The functions  $Z_{\sigma}^{\perp}$  and  $Z_{\pi}^{\perp}$  are the wave-function renormalizations of the sigma field and pion field perpendicular to the heat bath. The definition of the momentum dependent boson propagator  $P_B$  can be found in App. A. The masses  $M_i$  of the scalar fields are in



general momentum dependent,  $\bar{M}_i = \bar{M}_i(p_0, \{p_i\})$ , and given by the eigenvalues of the second derivative matrix of the potential,

$$\bar{M}_{ij}(\Phi, p, q) = \frac{\overrightarrow{\delta}}{\delta(\delta\Phi_i^T(-p))} \int d^4x U(\Phi + \delta\Phi) \frac{\overleftarrow{\delta}}{\delta(\delta\Phi_j(q))} \quad \text{with} \quad \delta\Phi^T = (\delta\Phi_1^T, \delta\Phi_2^T), \quad (8)$$

evaluated at the scalar background-field configuration  $\Phi$ . In the following, we approximate the full potential  $U$  by a Taylor expansion in terms of the fields around the physical ground-state  $\Phi_0$  up to quartic order<sup>4</sup>. Note that such a low-order expansion of the chiral order-parameter potential is incapable of describing a first-order phase transition. In particular, we are not able to detect the emergence a critical endpoint. However, our present work can be generalized straightforwardly along the lines of Refs. [61] or [28] where first-order transitions have been studied within RG approaches.

In the regime with an  $O(2)$  symmetric ground-state ( $\Phi_0 = 0$ ), we use

$$U_{\text{sym}}(\Phi) = \frac{1}{2}m^2\Phi^2 + \frac{\bar{\lambda}_\phi}{4}\Phi^4. \quad (9)$$

In this case, the masses of the scalar fields are given by

$$\bar{M}_\sigma^2(\Phi) = 2\frac{\partial U_{\text{sym}}}{\partial\Phi^2} + 4\Phi^2\frac{\partial^2 U_{\text{sym}}}{\partial\Phi^2\partial\Phi^2} = m^2 + 3\bar{\lambda}_\phi\Phi^2, \quad (10)$$

$$\bar{M}_\pi^2(\Phi) = 2\frac{\partial U_{\text{sym}}}{\partial\Phi^2} = m^2 + \bar{\lambda}_\phi\Phi^2, \quad (11)$$

and the physical masses  $M_i(\Phi = 0)$  are degenerate. In the regime with spontaneously broken  $O(2)$  symmetry of the ground-state ( $\langle\Phi\rangle \equiv \Phi_0 \neq 0$ ), we use the ansatz

$$U_{\text{bro}}(\Phi) = \frac{\bar{\lambda}_\phi}{4}(\Phi^2 - \Phi_0^2)^2, \quad (12)$$

which yields

$$\bar{M}_\sigma^2(\Phi) = 2\frac{\partial U_{\text{bro}}}{\partial\Phi^2} + 4\Phi^2\frac{\partial^2 U_{\text{bro}}}{\partial\Phi^2\partial\Phi^2} = \bar{\lambda}_\phi(\Phi^2 - \Phi_0^2) + 2\bar{\lambda}_\phi\Phi^2, \quad (13)$$

$$\bar{M}_\pi^2(\Phi) = 2\frac{\partial U_{\text{bro}}}{\partial\Phi^2} = \bar{\lambda}_\phi(\Phi^2 - \Phi_0^2). \quad (14)$$

for the masses of the scalar fields.

---

<sup>4</sup> We neglect higher-order terms since we are not aiming at a high-accuracy determination of critical exponents, where such higher-order terms have proven their importance, see e. g. [37, 59, 60]

The fermionic contribution  $U_F$  to the effective potential  $U$  reads

$$U_F(\Phi) = 2N_c T \sum_{n=-\infty}^{\infty} \int \frac{d^3p}{(2\pi)^3} \bar{p}^2 (\partial_t r_{\psi,k}) \left\{ Z_{\psi}^{\perp}(\nu_n, \{p_i\}) \mathcal{P}^{(+)}(\bar{M}_{\psi}) \right. \\ \left. + Z_{\psi}^{\perp}(-\nu_n, \{-p_i\}) \mathcal{P}^{(-)}(\bar{M}_{\psi}) \right\}, \quad (15)$$

where  $\nu_n = (2n+1)\pi T$  denotes the fermionic Matsubara frequencies and the fermion mass is given by

$$\bar{M}_{\psi}^2 \equiv \bar{M}_{\psi}^2(\nu_n, \{p_i\}) = \frac{1}{2}(\bar{h}(\nu_n, \{p_i\}))^2 \Phi^2. \quad (16)$$

The fermion propagators  $\mathcal{P}^{\pm}$  are defined in App. A. As we shall see in Sec. II B, the wave-function renormalizations  $Z_{\psi}^{\perp}$  and  $Z_{\psi}^{\parallel}$  and the fermion mass have the property

$$(Z_{\psi}^{\perp}(\nu_n, \{p_i\}))^* = Z_{\psi}^{\perp}(-\nu_n, \{p_i\}), \quad (Z_{\psi}^{\parallel}(\nu_n, \{p_i\}))^* = Z_{\psi}^{\parallel}(-\nu_n, \{p_i\}) \\ \text{and } (\bar{M}_{\psi}(\nu_n, \{p_i\}))^* = \bar{M}_{\psi}(-\nu_n, \{p_i\}). \quad (17)$$

Thus the fermion propagator obeys

$$(\mathcal{P}^{(+)}(\bar{M}_{\psi}(\nu_n, \{p_i\})))^* = \mathcal{P}^{(-)}(\bar{M}_{\psi}(-\nu_n, \{p_i\})) \quad (18)$$

and the fermionic contribution  $U_F$  to the effective potential is *real-valued*, as it should be:

$$U_F(\Phi) = 8N_c T \mathbf{Re} \sum_{n=0}^{\infty} \int \frac{d^3p}{(2\pi)^3} \bar{p}^2 (\partial_t r_{\psi,k}) Z_{\psi}^{\perp}(\nu_n, \{p_i\}) \mathcal{P}^{(+)}(\bar{M}_{\psi}). \quad (19)$$

The fact that  $U_F$ , and thus  $U$ , is real-valued is an important property of the effective potential, since it can then be expanded in powers of  $\mu^2/(\pi^2 T^2)$ . As a consequence, we can expand the phase boundary in powers of  $\mu^2/(\pi T)^2$  around  $\mu = 0$ .

The RG flow equations for the couplings  $m^2$ ,  $\lambda_{\phi}$  and the vacuum expectation value  $\Phi_0$  can now be calculated by projecting the RHS of Eqs. (7) and (15) onto our ansätze (9) and (12) for the potential  $U$ . In order to study the RG flow of the potential, we introduce the following dimensionless renormalized quantities:

$$\epsilon = \frac{m^2}{Z_{\phi}^{\perp} k^2}, \quad \lambda_{\phi} = \frac{\bar{\lambda}_{\phi}}{(Z_{\phi}^{\perp})^2}, \quad \kappa = \frac{1}{2} \frac{Z_{\phi}^{\perp} \Phi_0^2}{k^2}, \quad h^2 = \frac{\bar{h}^2}{Z_{\phi}^{\perp} (Z_{\psi}^{\perp})^2}. \quad (20)$$

For the symmetric regime, we then find (with  $v_3 = \frac{1}{8\pi^2}$ )

$$\partial_t \epsilon = (\eta_{\phi}^{\perp} - 2)\epsilon - 8v_3 \lambda_{\phi} l_1^{(B),(4)}(\tilde{t}, \epsilon; \eta_{\phi}^{\perp}) + 8N_c v_3 h^2 l_1^{(F),(4)}(\tilde{t}, 0, \tilde{\mu}; \eta_{\psi}^{\perp}), \quad (21)$$

$$\partial_t \lambda_{\phi} = 2\eta_{\phi}^{\perp} \lambda_{\phi} + 20v_3 \lambda_{\phi}^2 l_2^{(B),(4)}(\tilde{t}, \epsilon; \eta_{\phi}^{\perp}) - 8N_c v_3 h^4 l_2^{(F),(4)}(\tilde{t}, 0, \tilde{\mu}; \eta_{\psi}^{\perp}), \quad (22)$$

where  $\tilde{t} = T/k$  and  $\tilde{\mu} = \mu/k$  denote the dimensionless temperature and dimensionless chemical potential. The anomalous dimensions  $\eta_\phi^\perp$  of the scalar and  $\eta_\psi^\perp$  of fermion field are given by

$$\eta_\phi^\perp = -\partial_t \ln Z_\phi^\perp \quad \text{and} \quad \eta_\psi^\perp = -\partial_t \ln Z_\psi^\perp. \quad (23)$$

For the regime with broken O(2) symmetry in the ground-state, we find the following flow equations:

$$\begin{aligned} \partial_t \kappa &= -(\eta_\phi^\perp + 2)\kappa + 6v_3 l_1^{(B),(4)}(\tilde{t}, 2\kappa\lambda_\phi; \eta_\phi^\perp) + 2v_3 l_1^{(B),(4)}(\tilde{t}, 0; \eta_\phi^\perp) \\ &\quad - 8N_c v_3 \frac{h^2}{\lambda_\phi} l_1^{(F),(4)}(\tilde{t}, \kappa h^2, \tilde{\mu}; \eta_\psi^\perp), \quad (24) \\ \partial_t \lambda_\phi &= 2\eta_\phi^\perp \lambda_\phi + 18v_3 \lambda_\phi^2 l_2^{(B),(4)}(\tilde{t}, 2\kappa\lambda_\phi; \eta_\phi^\perp) + 2v_3 \lambda_\phi^2 l_2^{(B),(4)}(\tilde{t}, 0; \eta_\phi^\perp) \\ &\quad - 8N_c v_3 h^4 l_2^{(F),(4)}(\tilde{t}, \kappa h^2, \tilde{\mu}; \eta_\psi^\perp). \quad (25) \end{aligned}$$

The threshold functions are defined in App. B and can be represented as Feynman diagrams associated with purely bosonic and fermionic loops involving the corresponding full propagators. The regulator dependence of the flow equations is absorbed into these functions.

## B. RG Flow of the Yukawa coupling

We now turn to the calculation of the flow equation of the Yukawa coupling. Expanding the flow equation up to second order in the fermionic fields, we find at  $T = 0$  and  $\mu = 0$  [62]:

$$\begin{aligned} \delta\Gamma_{k,\bar{\psi}\psi}^{(2)} &= \frac{1}{4} \int \frac{d^4 q}{(2\pi)^4} \tilde{\partial}_t \left\{ \left[ \bar{h}\left(\frac{q_0 + Q_0}{2}, \left\{\frac{q_i + Q_i}{2}\right\}\right) \right]^2 \bar{\psi} P_\psi^{(+)}(\bar{M}_\psi) P_{B,\sigma}(Q_0 - q_0, \{Q_i - q_i\}) \psi \right. \\ &\quad \left. - \left[ \bar{h}\left(\frac{Q_0 - q_0}{2}, \left\{\frac{Q_i - q_i}{2}\right\}\right) \right]^2 \bar{\psi} P_\psi^{(-)}(\bar{M}_\psi) P_{B,\sigma}(Q_0 + q_0, \{Q_i + q_i\}) \psi \right\} \\ &\quad - (P_{B,\sigma} \rightarrow P_{B,\pi}), \quad (26) \end{aligned}$$

where  $Q_\mu$  denotes the four-momenta of an incoming fermion. The flow equation for the Yukawa coupling  $\bar{h}(Q_0, \{Q_i\})$  is obtained from this expression by projecting it onto the operator  $\frac{1}{\sqrt{2}}(\bar{\psi} \vec{\tau} \cdot \Phi \psi)$ .

For finite temperature  $T$ , the integral in  $q_0$ -direction becomes a sum over Matsubara frequencies. Let us now discuss this integral/sum in Euclidean time direction in Eq.(26). Since we use a 3d regulator, we can study the integral/sum in Euclidean time direction without discussing details of the regulator function or of the integration in spatial directions.

As a first approximation [62], we set  $q_0 \rightarrow Q_0$  and  $q_i \rightarrow Q_i$  in the argument of the fermion mass and the Yukawa coupling on the RHS of Eq. (26) and take then the limit of vanishing spatial external momenta  $Q_i \rightarrow 0$ . As we shall discuss further in the next subsection, we also neglect a possible difference between  $Z_{\psi,B}^\perp$  and  $Z_{\psi,B}^\parallel$ , thus  $Z_{\psi,B} \equiv Z_{\psi,B}^\perp = Z_{\psi,B}^\parallel$ . We then obtain the following expression for  $\delta\Gamma_{k,\bar{\psi}\psi}^{(2)}$ :

$$\delta\Gamma_{k,\bar{\psi}\psi}^{(2)} = \frac{(\bar{\psi}\vec{\tau} \cdot \Phi\psi)}{2\sqrt{2}} \int \frac{d^3q}{(2\pi)^3} \tilde{\partial}_t \delta\tilde{\Gamma}_{k,\bar{\psi}\psi}^{(2)}(\{q_i\}, Q_0, 0) + (P_{B,2} \rightarrow P_{B,1}), \quad (27)$$

with

$$\begin{aligned} & Z_\phi^{-\frac{1}{2}} Z_\psi^{-1} \left( \delta\tilde{\Gamma}_{k,\bar{\psi}\psi}^{(2)}(\{q_i\}, Q_0, 0) \right) \\ &= [h(Q_0, 0)]^3 \int \frac{dq_0}{2\pi} \frac{1}{\bar{q}^2(1+r_\psi)^2 + (q_0 + i\mu)^2 + M_\psi^2(Q_0, 0)} \frac{1}{\bar{q}^2(1+r_B) + (Q_0 - q_0)^2 + M_{B,2}^2} \end{aligned} \quad (28)$$

and  $M_B^2 = \bar{M}_B^2/Z_\phi$  and  $M_\psi^2 = \bar{M}_\psi^2/Z_\psi$ .

Let us first consider the case of finite chemical potential but zero temperature. In this case we observe that Eq. (28) is a real number if and only if  $Q_0$  is zero. This can be seen by writing the fermion propagator as follows:

$$\frac{1}{\bar{q}^2(1+r_\psi)^2 + (q_0 + i\mu)^2 + M_\psi^2(Q_0, 0)} = \frac{\bar{q}^2(1+r_\psi)^2 + M_\psi^2(Q_0, 0) + q_0^2 - \mu^2 - 2iq_0\mu}{|\bar{q}^2(1+r_\psi)^2 + (q_0 + i\mu)^2 + M_\psi^2(Q_0, 0)|^2}. \quad (29)$$

Thus the imaginary part of the fermion propagator is linear in  $q_0$  and vanishes by integration for  $Q_0 \rightarrow 0$ . This means, however, that the Yukawa coupling becomes a complex number for a finite external time-like momenta  $Q_0$  since in this case the integrand in Eq. (28) is no longer symmetric in  $q_0$ .

Now we switch on temperature. Since  $Q_0$  is the Euclidean time component of an incoming fermion, we have  $Q_0 = (2m+1)\pi T \equiv \nu_m$ . Taking into account that the integral in Eq. (28) runs over fermionic momenta ( $q_0 = (2n+1)\pi T \equiv \nu_n$ ), we find

$$\begin{aligned} & Z_\phi^{-\frac{1}{2}} Z_\psi^{-1} \left( \delta\tilde{\Gamma}_{k,\bar{\psi}\psi}^{(2)}(\{q_i\}, \nu_m, 0) \right) \\ &= [h(\nu_m, 0)]^3 T \sum_{n=-\infty}^{\infty} \frac{1}{\bar{q}^2(1+r_\psi)^2 + (\nu_n + i\mu)^2 + M_\psi^2(\nu_m, 0)} \frac{1}{\bar{q}^2(1+r_B) + (\nu_m - \nu_n)^2 + M_{B,2}^2}. \end{aligned} \quad (30)$$

Since  $\nu_m - \nu_n = 2(m-n)\pi T$  is effectively a bosonic Matsubara frequency, the sum over  $n$  is not symmetric in  $n$  and we find that the RHS is in general a *complex* number for any given value of  $m$ , and so is the Yukawa coupling and the fermion mass. From Eq. (30), we

conclude

$$(h(\nu_m, 0))^* = h(-\nu_m, 0), \quad (31)$$

and equivalently for the fermion mass. Thus we have found that the Yukawa coupling for a given external momenta is in general complex-valued when evaluated at a finite quark chemical potential. This is not an issue as long as we take the full momentum dependence of the Yukawa coupling into account, as we have argued in Sec. II A. In the following we shall restrict ourselves to a momentum-independent Yukawa coupling which has been successfully employed in studies of the quark-meson model with two quark flavors at vanishing chemical potential, see e. g. Ref. [41, 42, 62]. This requires care in finding a proper approximation scheme that gives us a real-valued effective potential  $U$  without computing the full momentum dependence of the couplings. The idea for constructing such a scheme is to expand the theory around the limit  $\pi T/k \rightarrow 0$  of vanishing external momenta. This might appear dangerous for  $k \lesssim \pi T$ , but what comes to our rescue is the fact that  $\pi T/k \lesssim 1/2$  above the scale  $k_{\chi SB}$  at which QCD enters the chirally broken regime. For scales  $k < k_{\chi SB}$ , the fermions acquire a mass due to the presence of a quark condensate and therefore the fermionic contributions to the flow decouple rapidly anyway. Thus, once chiral symmetry is broken, our approximation in the fermionic subsector should not influence our results much. For the purpose of implementing this truncation scheme, we introduce the following dimensionless quantities:

$$x^2 = \frac{\vec{q}^2}{k^2}, \quad \tilde{\nu}_n = \frac{\nu_n}{k} \quad \text{and} \quad m_{\psi, B}^2 = \frac{M_{\psi, B}^2}{k^2}. \quad (32)$$

Now we rewrite Eq. (30) in terms of dimensionless propagators:

$$\begin{aligned} & Z_\phi^{-\frac{1}{2}} Z_\psi^{-1} \left( k \delta \tilde{\Gamma}_{k, \psi \bar{\psi}}^{(2)}(\{q_i\}, \tilde{\nu}_m, 0) \right) \\ &= [h(\tilde{\nu}_m, 0)]^3 \tilde{t} \sum_{n=-\infty}^{\infty} \frac{1}{x^2(1+r_\psi)^2 + (\tilde{\nu}_n + i\tilde{\mu})^2 + m_\psi^2(\tilde{\nu}_m, 0)} \frac{1}{x^2(1+r_B) + (\tilde{\nu}_m - \tilde{\nu}_n)^2 + m_{B,2}^2}. \end{aligned} \quad (33)$$

Assuming that  $\tilde{\nu}_m$  is a small parameter, we can expand the boson propagator in powers of  $\nu_m$ :

$$\begin{aligned} & \frac{1}{x^2(1+r_B) + (\tilde{\nu}_m - \tilde{\nu}_n)^2 + m_B^2} \\ &= \frac{1}{x^2(1+r_B) + \tilde{\nu}_n^2 + m_B^2} \left( 1 + \frac{2\tilde{\nu}_n \tilde{\nu}_m}{x^2(1+r_B) + \tilde{\nu}_n^2 + m_B^2} + \mathcal{O}(\tilde{\nu}_m^2) \right). \end{aligned} \quad (34)$$

Equivalently, we expand the Yukawa coupling and the masses:

$$h(\tilde{\nu}_m, 0) = h + h^{(1)}\tilde{\nu}_m + \mathcal{O}(\tilde{\nu}_m^2), \quad (35)$$

$$m_{\psi,B}(\tilde{\nu}_m, 0) = m_{\psi,B} + m_{\psi,B}^{(1)}\tilde{\nu}_m + \mathcal{O}(\tilde{\nu}_m^2). \quad (36)$$

Keeping only the zeroth order in these expansions, we obtain for  $\delta\tilde{\Gamma}_{k,\bar{\psi}\psi}^{(2)}(\{q_i\}, \tilde{\nu}_m, 0)$ :

$$\begin{aligned} & Z_\phi^{-\frac{1}{2}} Z_\psi^{-1} \left( k \delta\tilde{\Gamma}_{k,\bar{\psi}\psi}^{(2)}(\{q_i\}, \tilde{\nu}_m, 0) \right) \\ &= h^3 \tilde{t} \sum_{n=-\infty}^{\infty} \frac{1}{x^2(1+r_\psi)^2 + (\tilde{\nu}_n + i\tilde{\mu})^2 + m_\psi^2} \frac{1}{x^2(1+r_B) + \tilde{\nu}_n^2 + m_{B,2}^2}. \end{aligned} \quad (37)$$

We observe that this expression is a real number for all  $\tilde{\mu}$ . Thus a Taylor expansion of this expression around  $\tilde{\mu} = 0$  generates only terms with even powers in  $\tilde{\mu}$ .

Inserting Eq. (37) into Eq. (27) and incorporating the gluons in the same way as discussed here for the scalar fields, we obtain the final result for the flow of the Yukawa coupling:

$$\begin{aligned} \partial_t h^2 &= (\eta_\phi + 2\eta_\psi)h^2 - 4v_3 h^4 \left\{ L_{1,1}^{(FB),(4)}(\tilde{t}, \kappa h^2, \tilde{\mu}, m_\pi^2; \eta_\psi, \eta_\phi) - L_{1,1}^{(FB),(4)}(\tilde{t}, \kappa h^2, \tilde{\mu}, m_\sigma^2; \eta_\psi, \eta_\phi) \right\} \\ &\quad - 32v_3 g^2 h^2 C_2(N_c) \left\{ L_{1,1}^{(FB),(4)}(\tilde{t}, \kappa h^2, \tilde{\mu}, 0; \eta_\psi, \eta_F) - \frac{1-\xi}{3} \mathcal{L}_{1,1}^{(FB),(4)}(\tilde{t}, \kappa h^2, \tilde{\mu}, 0; \eta_\psi, \eta_F) \right\}, \end{aligned} \quad (38)$$

where  $\eta_F = -\partial_t \ln Z_F$ . Moreover, we have  $(m_\pi^2 = \epsilon, m_\sigma^2 = 2\kappa\lambda_\phi)$  in broken regime and  $m_\pi^2 = m_\sigma^2 = \epsilon$  in the symmetric regime. The threshold functions associated with triangle diagrams are defined in App. B. We have checked that our results agree with those in Ref. [30] in the limit  $T \rightarrow 0$  and  $\mu \rightarrow 0$  if we use a four-dimensional regulator function.

### C. RG Flow of the wave-function renormalizations

The flow equations for the fermionic wave-function renormalization can be extracted from the RHS of Eq. (26) along the lines of the calculation of the Yukawa coupling. Projecting Eq. (26) onto  $\bar{\psi}(-\gamma_i Q_i)\psi$  and then taking the limit  $Q_0 \rightarrow 0$  and  $Q_i \rightarrow 0$ , we obtain the flow of  $Z_\psi^\perp$ :

$$\begin{aligned} \eta_\psi^\perp &= \frac{4v_3}{3} C_2(N_c) g^2 \left\{ 4 \mathcal{M}_{1,2}^{(FB),(4)}(\tilde{t}, \kappa h^2, \tilde{\mu}, 0, 0) - 8(1-\xi) \tilde{\mathcal{N}}_{1,1,1}^{(FB),(4)}(\tilde{t}, \kappa h^2, \tilde{\mu}, 0, 0) \right. \\ &\quad \left. + \frac{12}{5}(1-\xi) \left( \mathcal{N}_{1,2}^{(FB),(4)}(\tilde{t}, \kappa h^2, \tilde{\mu}, 0, 0) + \tilde{\mathcal{N}}_{1,1,2}^{(FB),(4)}(\tilde{t}, \kappa h^2, \tilde{\mu}, 0, 0) \right) \right\} \\ &\quad + \frac{4v_3}{3} h^2 \left\{ \left( \mathcal{M}_{1,2}^{(FB),(4)}(\tilde{t}, \kappa h^2, \tilde{\mu}, m_\sigma^2, 0) + \mathcal{M}_{1,2}^{(FB),(4)}(\tilde{t}, \kappa h^2, \tilde{\mu}, m_\pi^2, 0) \right) \right\}, \end{aligned} \quad (39)$$

where the corresponding threshold functions can be found in App. B. Note that we do not display the dependence of the threshold functions on the anomalous dimensions  $\eta_\phi^\perp$  of the scalars,  $\eta_\psi^\perp$  of the fermions and  $\eta_F$  of the gluons for brevity, but we take it into account in the numerical evaluation of the flow equations. We find agreement with the equation for  $\eta_\psi$  in Ref. [30] in the limit  $T \rightarrow 0$  and  $\mu \rightarrow 0$  if we use a four-dimensional regulator function. A flow equation for  $Z_\psi^\parallel(Q_0, \{Q_i\})$  could in principle be obtained in the same manner by projecting Eq. (26) onto  $\bar{\psi}(-\gamma_0 Q_0)\psi$ .

The derivation of the scalar wave-function renormalization can be performed along the lines of Refs. [30, 37, 62]. Projecting the flow equation onto  $\phi\vec{p}^2\phi$  and taking the limit of  $Q_0 = 0$  and  $Q_i = 0$  for the external momenta, we find the wave-function renormalization  $Z_\phi^\perp$ :

$$\begin{aligned} \eta_\phi^\perp = & \frac{16v_3}{3}\kappa\lambda_\phi^2\mathcal{M}_{2,2}^{(B),(4)}(\tilde{t}, m_\sigma^2, m_\pi^2; \eta_\phi^\perp) + \frac{40v_3}{9}N_ch^2\mathcal{M}_4^{(F),(4)}(\tilde{t}, \kappa h^2, \tilde{\mu}; \eta_\psi^\perp) \\ & + \frac{16v_3}{3}N_ch^4\kappa\mathcal{M}_2^{(F),(4)}(\tilde{t}, \kappa h^2, \tilde{\mu}; \eta_\psi^\perp). \end{aligned} \quad (40)$$

The threshold functions are defined in App. B. For vanishing temperature and quark chemical potential, we find that the equation for  $\eta_\phi^\perp$  agrees with the equation for  $\eta_\phi$  provided we employ a four-dimensional regulator function.

Here and in the following we neglect that  $Z_\phi^\parallel \neq Z_\phi^\perp$  and  $Z_\psi^\parallel \neq Z_\psi^\perp$  and work in the approximation  $Z_\phi^\parallel = Z_\phi^\perp$  and  $Z_\psi^\parallel = Z_\psi^\perp$ . For our purposes, this is justified since we are only interested in chiral symmetry breaking in QCD but not in a calculation of thermodynamical quantities above  $T_c$ . For scales  $k > k_{\chi SB}$ , we have  $Z_i^\parallel \approx Z_i^\perp$  since  $T/k < 1$ . For scales  $k \ll T$ , we approach the three-dimensional limit and the RG flow is driven only by the lowest Matsubara modes. Since the lowest Matsubara frequency for the bosons is zero, the dependence of the propagators on  $Z_\phi^\parallel$  drops out, see App. A for our definition of the propagators. In case of the fermions the lowest Matsubara frequency is proportional to the temperature  $T$ . Therefore the fermions effectively decouple from the RG flow for  $k \ll T$  and our approximation  $Z_\psi^\parallel \neq Z_\psi^\perp$  hardly affects the RG flow. Overall, the distinction of  $Z_i^\parallel$  and  $Z_i^\perp$  plays only a quantitatively important role for temperatures  $T > T_c$ : There the mid-momentum regime is not protected by a dynamically generated mass gap from chiral symmetry breaking and modes with  $k \sim T$  can actually probe the difference between  $Z_i^\parallel$  and  $Z_i^\perp$ .

### D. RG Flow of the four-fermion interaction

The flow equation for the four-fermion interaction  $\bar{\lambda}_\sigma$  can be obtained as well by projecting the expansion (5) of the RG flow equation onto our ansatz (1) for the effective action. In anticipation of what follows, we note that we only need to take contributions arising from the fourth order term in the expansion (5) into account. These are contributions from so-called one-particle irreducible (1PI) "box"-diagrams. As we shall see in Sec. II E, we do not need to compute 1PI four-fermion self-interaction diagrams ( $\sim \bar{\lambda}_\sigma^2$ ) and so-called 1 PI "triangle"-diagrams ( $\sim \bar{\lambda}_\sigma \bar{g}^2$  and  $\sim \bar{\lambda}_\sigma \bar{h}^2$ ), even though these diagrams would contribute to the RG flows of the four-fermion couplings in a non-rebosonized study [31, 32, 43, 63]. As a consequence, it is sufficient to consider the limit  $\bar{\lambda}_\sigma \rightarrow 0$  on the RHS of the flow equation of  $\bar{\lambda}_\sigma$ . We find:

$$\partial_t \bar{\lambda}_\sigma \Big|_{\bar{\lambda}_\sigma \rightarrow 0} = \frac{Z_\psi^2}{k^2} \left( \beta_{\bar{\lambda}_\sigma}^{g^4} g^4 + \beta_{\bar{\lambda}_\sigma}^{h^4} h^4 \right) \quad (41)$$

with

$$\beta_{\bar{\lambda}_\sigma}^{h^4} = \frac{1}{2N_c} \frac{4v_3}{3} \left( L_{1,1,1,1}^{(FB),(4)}(\tilde{t}, \kappa h^2, \tilde{\mu}, \tilde{\mu}, m_\sigma^2, m_\pi^2) + L_{1,1,1,1}^{(FB),(4)}(\tilde{t}, \kappa h^2, \tilde{\mu}, -\tilde{\mu}, m_\sigma^2, m_\pi^2) \right), \quad (42)$$

$$\beta_{\bar{\lambda}_\sigma}^{g^4} = -\frac{21 (C_2(N_c))^2}{2N_c} \frac{4v_3}{3} \left( L_{1,1,1,1}^{(FB),(4)}(\tilde{t}, \kappa h^2, \tilde{\mu}, \tilde{\mu}, 0, 0) + L_{1,1,1,1}^{(FB),(4)}(\tilde{t}, \kappa h^2, \tilde{\mu}, -\tilde{\mu}, 0, 0) \right). \quad (43)$$

The threshold functions can be found in App. B. We do not display the dependence of the threshold functions on the anomalous dimensions of the corresponding fields for brevity but we take it into account in the numerical evaluation of the flow equations.

We have chosen the same Fierz transformations in the Dirac algebra as in Refs. [29, 30]. In the present study we discard additional four-fermion interactions of the type  $(\bar{\psi} \gamma_0 \psi)^2$  which are generated in the finite-temperature RG flows. However, such interactions are suppressed for scales  $k > T$  compared to the included four-fermion interaction anyway. We have also neglected four-fermion interactions, such as a vector-channel, in our truncation of the effective action. Therefore our results for the phase boundary will depend slightly on our choice of Fierz-transformation with respect to Dirac and color indices. However, it has been checked in Ref. [30] that results for low-energy observables at zero temperature obtained in different Fierz decompositions involving a color-singlet scalar-pseudoscalar channel agree on the 1% percent level. We would like to stress that it is possible to fully resolve such a Fierz



ambiguity in larger truncations within the functional RG approach [31, 32, 43] even when "re-bosonization" techniques are applied [29, 63, 64].

### E. RG Flow of the rebosonized couplings

Let us now briefly discuss the so-called "re-bosonization" procedure which we apply in order to resolve the redundancy in our ansatz for the effective action (1). The redundancy originates from the fact that a Yukawa coupling together with a bosonic potential can be transformed into a four-fermion interaction and vice versa. In order to lift this redundancy we work along the lines of Ref. [30] and allow for  $k$ -dependent scalar fields  $\Phi_{1,k}$  and  $\Phi_{2,k}$ . The flow equation (3) changes then as follows [29, 30]:

$$\partial_t \Gamma_k = \partial_t \Gamma_k \Big|_{\Phi_k} + \int \frac{d^4 q}{(2\pi)^4} \left( \frac{\delta \Gamma_k}{\delta \Phi_{1,k}} \partial_t \Phi_{1,k} + \frac{\delta \Gamma_k}{\delta \Phi_{2,k}} \partial_t \Phi_{2,k} \right), \quad (44)$$

where the first term on the RHS is simply the flow equation (3) for fixed fields  $\Phi_{1,k}$  and  $\Phi_{2,k}$  and the second term takes care of the fact that the scalar fields change under a variation of the RG scale  $k$ . In the following, we span the RG flow of the scalar fields  $\Phi_{1,k}$  and  $\Phi_{2,k}$  by the corresponding field itself and a fermionic composite operator with the same quantum numbers:

$$\partial_t \Phi_{1,k} = \frac{1}{\sqrt{2}} (\bar{\psi} \gamma_5 \psi) \partial_t \alpha_k + \Phi_{1,k} \partial_t \beta_k, \quad (45)$$

$$\partial_t \Phi_{2,k} = \frac{i}{\sqrt{2}} (\bar{\psi} \psi) \partial_t \alpha_k + \Phi_{2,k} \partial_t \beta_k. \quad (46)$$

The functions  $\alpha_k$  and  $\beta_k$  determine the transformation of the scalar fields under the RG flow and can be derived unambiguously from enforcing several conditions: The flow of  $\bar{\lambda}_\sigma(q^2)$  must vanish on all scales  $k$  and for all  $q^2$ , the Yukawa coupling must be momentum independent and the flow of the wave-function renormalization of the scalar fields must obey  $\partial_t Z_\phi(q^2 = k^2) = -\eta_\phi Z_\phi$ , see Refs. [29, 30] for details. Using the initial condition  $\bar{\lambda}_\sigma|_{k \rightarrow \Lambda} = 0$  for the four-fermion coupling at the UV cutoff scale  $\Lambda$ , the first condition ensures that no coupling  $\bar{\lambda}_\sigma$  is generated in the RG flow. We stress that it is this "re-bosonization" procedure which allows us to bridge the gap between the perturbative quark-gluon regime in the UV and the regime dominated by massless Goldstone modes in the IR without performing any additional fine tuning. From a technical point of view, this technique allows us to include

(momentum-dependent) four-fermion interactions up to arbitrary order, provided we do not truncate our ansatz for the scalar potential  $U(\Phi^2)$ .

By applying the field transformations (45) and (46), we modify the flow equations for scalar couplings. We find for the flow equations in the symmetric regime:

$$\partial_t \epsilon = \partial_t \epsilon \Big|_{\Phi_k} + 2 \frac{\epsilon(1+\epsilon)}{h^2} ((1+\epsilon)Q_\sigma + 1) \left( \beta_{\bar{\lambda}_\sigma}^{g^4} g^4 + \beta_{\bar{\lambda}_\sigma}^{h^4} h^4 \right), \quad (47)$$

$$\partial_t h^2 = \partial_t h^2 \Big|_{\Phi_k} + 2 \left( (1+\epsilon)^2 Q_\sigma + 1 + 2\epsilon \right) \left( \beta_{\bar{\lambda}_\sigma}^{g^4} g^4 + \beta_{\bar{\lambda}_\sigma}^{h^4} h^4 \right), \quad (48)$$

$$\partial_t \lambda_\phi = \partial_t \lambda_\phi \Big|_{\Phi_k} + 4 \frac{\lambda_\phi}{h^2} (1+\epsilon) (1 + (1+\epsilon)Q_\sigma) \left( \beta_{\bar{\lambda}_\sigma}^{g^4} g^4 + \beta_{\bar{\lambda}_\sigma}^{h^4} h^4 \right). \quad (49)$$

Similarly we obtain the following set of flow equations in the regime with broken  $O(2)$  symmetry:

$$\partial_t \kappa = \partial_t \kappa \Big|_{\Phi_k} + 2 \frac{\kappa(1-\kappa\lambda_\phi)}{h^2} ((1+\kappa\lambda_\phi)Q_\sigma + 1) \left( \beta_{\bar{\lambda}_\sigma}^{g^4} g^4 + \beta_{\bar{\lambda}_\sigma}^{h^4} h^4 \right), \quad (50)$$

$$\partial_t h^2 = \partial_t h^2 \Big|_{\Phi_k} + 2 \left( (1-\kappa\lambda_\phi)^2 Q_\sigma + 1 - 2\kappa\lambda_\phi \right) \left( \beta_{\bar{\lambda}_\sigma}^{g^4} g^4 + \beta_{\bar{\lambda}_\sigma}^{h^4} h^4 \right), \quad (51)$$

$$\partial_t \lambda_\phi = \partial_t \lambda_\phi \Big|_{\Phi_k} + 4 \frac{\lambda_\phi}{h^2} (1-\kappa\lambda_\phi) (1 + (1-\kappa\lambda_\phi)Q_\sigma) \left( \beta_{\bar{\lambda}_\sigma}^{g^4} g^4 + \beta_{\bar{\lambda}_\sigma}^{h^4} h^4 \right). \quad (52)$$

The function  $Q_\sigma$  occuring in the equations for the symmetric and the broken regime measures the suppression of the four-fermion interaction for large momenta, which we treat in an  $s$ -channel approximation. It is defined as [29, 30]:

$$Q_\sigma(T, \mu, \bar{M}_\psi) := \frac{\partial_t (\bar{\lambda}_\sigma(k^2, T, \mu, \bar{M}_\psi) - \bar{\lambda}_\sigma(0, T, \mu, \bar{M}_\psi))}{\partial_t \bar{\lambda}_\sigma(0, T, \mu, \bar{M}_\psi)}. \quad (53)$$

Note that  $Q_\sigma$  depends on the temperature  $T$ , the quark chemical potential  $\mu$  and the quark mass  $\bar{M}_\psi$ . In order to compute  $Q_\sigma$ , we would in principle need to compute the full momentum dependence of the four-fermion interaction. For simplicity, we do not perform an explicit computation of the momentum dependence but model it with the aid of theoretical constraints. First, we assume that  $Q_\sigma < 0$  in order to be consistent with unitarity at  $T = 0$ . Second, the four-fermion interaction in the  $s$  channel can be considered to be roughly point-like once the quarks acquire a mass. At finite temperature, the quarks acquire an additional thermal mass which further suppresses the momentum dependence. According to Ref. [30], we therefore model  $Q_\sigma$  by employing a threshold function that captures these constraints:

$$Q_\sigma(\tilde{t}, \tilde{\mu}, m_\psi) = Q_\sigma^0 \mathcal{M}_{1,2}^{(4),(FB)}(\tilde{t}, m_\psi^2, \tilde{\mu}, 0, 0; \eta_\psi, \eta_F). \quad (54)$$

Here,  $Q_\sigma^0$  is a negative constant at our disposal. We choose  $Q_\sigma^0 = -1$ , but we have checked that our results for the phase boundary and in particular for the curvature at small chemical potential change only on the 1% level when we vary  $Q_\sigma^0$  from  $Q_\sigma^0 = -1$  up to  $Q_\sigma^0 = -0.01$ .

### F. Running of the gauge coupling and gluonic anomalous dimension

Finally we need to discuss the running of the gauge coupling which is one of the key ingredients of our study of the QCD phase boundary. From now on we restrict our discussion to Landau-gauge QCD.

In this work, we use two ansätze for the running of the coupling in Landau-gauge QCD. This allows us to give a theoretical error estimate for our results. The first ansatz has been extensively discussed at both zero and finite temperature in Refs. [31, 32, 65]. It is based on the following truncation in the pure gluonic part of the effective action:

$$\Gamma_k^{\text{FE}} = \int_x \left\{ Z_k^{(1)} F_{\mu\nu}^a F_{\mu\nu}^a + Z_k^{(2)} (F_{\mu\nu}^a F_{\mu\nu}^a)^2 + \dots \right\}. \quad (55)$$

Such a calculation of the coupling employs the background-field formalism [66] within the RG framework [44, 65, 67, 68, 69, 70, 71, 72, 73].

The ansatz (55) for the pure gluonic part of the effective action used for the determination of the running coupling includes an infinite power series of the gauge-invariant operator  $F_{\mu\nu}^a F_{\mu\nu}^a$ . The truncation includes arbitrarily high gluonic correlators projected onto their small-momentum limit and onto the particular color and Lorentz structure arising from powers of  $F_{\mu\nu}^a F_{\mu\nu}^a$ . It represents a gradient expansion in the field strength to arbitrary order but neglects higher-derivative terms and more complicated color and Lorentz structures. Using the background-field method, the  $\beta$ -function of the running coupling  $g$  is related to the wave-function renormalization of the background field [66] via

$$\partial_t \alpha_{\text{FE}} = \eta_{\text{FE}} \alpha_{\text{FE}} \quad \text{with} \quad \eta_{\text{FE}} = -\partial_t \ln Z_k^{(1)} \equiv -\partial_t \ln Z_F^{\text{FE}}, \quad (56)$$

which is a consequence of the non-renormalization of the product of the background field and the bare coupling. The coefficient of the first term  $Z_k^{(1)} \equiv Z_F^{\text{FE}}/4$  in the effective action (55) evolves with the renormalization scale  $k$  and is successively driven by all other operators in the action. In Refs. [31, 65], the authors keep track of all contributions from the flows of the  $Z_k^{(i)}$  to the flow of the running coupling. An infrared fixed point for the running

coupling at zero temperature has been found in Ref. [65] with  $\alpha_{\text{FE}}^*(T=0) \in [5.7, 9.7]$ . The uncertainty arises from an unresolved color structure in the calculation. In the following we do not compute the running of the coupling from the truncation (55) explicitly but use the results from Refs. [31, 32] with  $\alpha_{\text{FE}}^*(T=0) = 5.7$ .

One of the main findings in Refs. [31, 32] is that the coupling exhibits a non-trivial infrared fixed point at finite temperature which has been recently confirmed by Lattice QCD simulations [74]. In the low momentum regime, the solution of the RG equations exhibits a linear behavior with a slope determined by the infrared fixed point  $\alpha_{3d}^*$  of the spatial 3d Yang-Mills theory [31, 32]:

$$\alpha_{\text{FE}}(k \ll T) \approx \alpha_{3d}^* \frac{k}{T} + \mathcal{O}\left(\left(\frac{k}{T}\right)^2\right). \quad (57)$$

The value of the infrared fixed point is given by  $\alpha_{3d}^* \approx 2.7$ . The actual presence of this finite infrared fixed point is important for temperatures around the chiral phase transition while the actual value of  $\alpha_{3d}^*$  is of less importance for a study of the chiral phase transition temperature<sup>5</sup>. Indeed, the running coupling obtained from the truncation (55) has been successfully used to determine the chiral phase boundary of QCD in the plane of temperature and number of massless quark flavors [31, 32].

Since our work relies partly on the background-field method, we would like to discuss briefly its advantages and disadvantages. The application of the background-field method to functional RG flow equations has been proposed in [67] and further developed in Refs. [44, 65, 67, 68, 69, 70, 71, 72, 73]. The background-field method provides a convenient framework for a study of gauge theories since it allows us in principle to construct a gauge-invariant effective action in a comparatively simple manner. The background-gauge fixing procedure [66] together with the regularization lead to regulator-modified Ward-Takahashi identities (mWTI) [68, 69, 70]. Here, we only employ an approximate solution to the flow in the gauge sector as obtained in Refs. [31, 32]. To be more specific, we identify the RG flows of the background field with those of the fluctuation field; for a treatment of the difference of both we refer to Ref. [71]. The identification of the background and fluctuation field results in a flow which is no longer closed and which does not satisfy all constraints

---

<sup>5</sup> The actual value of  $\alpha_{3d}^*$  may play an important role for the study of bulk thermodynamic quantities such as the pressure at high temperatures.

from the mWTI [44, 67, 68, 69, 70, 71, 72, 73]. In this work, we assume that the loss of information due to the identification of the background and the fluctuation field as well as corrections due to the mWTI are quantitatively small in the region of physical interest and do not severely affect our results, see Ref. [72]. The advantage of our approximations is that we obtain a gauge-invariant approximate solution of the theory. In the following we work in Landau-deWitt gauge whenever the background-field method is involved<sup>6</sup>. Since we shall also employ the coupling from lattice QCD in Landau gauge, our analysis of the phase boundary provides some quantitative insight into the quality of our approximations involved in the gauge-sector when treated within the background-field formalism.

In order to "measure" the impact of the gauge field dynamics on the QCD phase boundary and to estimate the theoretical error of our results arising from the truncation in the gauge sector, we also employ the running of the gauge coupling in Landau-gauge as measured on the Lattice in Ref. [77]. In Landau-gauge QCD, the running of the gauge coupling at vanishing temperature has been computed using lattice simulations [77, 78, 79, 80, 81], Dyson-Schwinger equations [82, 83, 84, 85] and functional RG methods [86, 87]. It can be defined by means of the ghost and the gluon propagator which is a consequence of the non-renormalization property of the ghost-gluon vertex [82, 83, 88]:

$$\alpha_{\text{Ref.}}(T=0, p^2) = \frac{\bar{g}^2}{4\pi Z_A(T=0, p^2) Z_C^2(T=0, p^2)}, \quad (58)$$

where  $Z_{A,C}$  denotes the dressing functions of the gluon and the ghost, respectively. The momentum dependence of the dressing functions are characterized by a power-law behavior in the deep IR [89]:

$$Z_A^{\text{IR}}(T=0, p^2) = (p^2)^{-2\kappa_C}, \quad Z_C^{\text{IR}}(T=0, p^2) = (p^2)^{\kappa_C}. \quad (59)$$

The exponents are related by the Landau-gauge sum rule in  $d=4$  dimensions [89, 90, 91]. In this work, we have suitably amended the lattice propagators in Ref. [77] by their perturbative behavior in the ultraviolet regime and the corresponding power laws in the IR. This yields an infrared fixed point  $\alpha_s(T=0) \approx 2.3$ .

For our finite temperature studies, we have adapted the running of the gauge coupling (58) such that it is governed by an infrared fixed point for momenta  $p \lesssim 2\pi T$  according to

---

<sup>6</sup> Note that Landau gauge is known to be a fixed point of the RG flow [75, 76]

the results in Refs. [31, 32]:

$$\alpha_{\text{Ref.}}(p \ll T) \approx \alpha_{3d}^* \frac{p}{T} + a_1 \left(\frac{p}{T}\right)^2 + a_2 \left(\frac{p}{T}\right)^3 + \dots \quad (60)$$

Here we drop all higher terms and choose  $\alpha_{3d}^* = 1$  and determine  $a_1$  and  $a_2$  such that the coupling (58) and its derivative with respect to  $p$  are connected continuously with the ansatz (60) at the scale set by the lowest non-vanishing bosonic Matsubara-mode  $\omega_T = 2\pi T$ . Although the actual values for  $a_1$ ,  $a_2$  and  $\alpha_{3d}^*$  may differ from the values chosen here, the arising uncertainties for the QCD phase boundary can be estimated by a comparison with the results obtained from the coupling defined in Eq. (56). In any case, the question whether the ground-state of QCD is governed by chiral symmetry breaking or not is controlled by the running of the coupling in the mid-momentum regime ( $0.5 \text{ GeV} \lesssim p \lesssim 1.5 \text{ GeV}$ ) as we shall see below. In this momentum regime, we have  $\alpha_{\text{Ref.}} > \alpha_{\text{FE}}$ .

From now on we identify the scale  $k^2$  set by the cutoff function with the momentum scale  $p^2$ . This nontrivial assumption is justified, because the regulator function which enters in the calculation of the running coupling specifies the Wilsonian momentum-shell integration in such a way that the RG flow of the coupling is dominated by fluctuations with momenta  $p^2 \approx k^2$ . For our calculation of the phase boundary, we need not only the strong coupling, but also the anomalous dimension  $\eta_F$  which we estimate from

$$\partial_t \alpha_{\text{Ref.}}(p^2 = k^2) = \eta_{\text{Ref.}} \alpha_{\text{Ref.}}(p^2 = k^2). \quad (61)$$

By estimating the gauge-field contributions to  $\eta_F = -\partial_t Z_F$  from  $\eta_{\text{Ref.}}$  and by using  $\alpha_{\text{Ref.}}$  in our calculations, we assume that the running of the coupling as found in Landau-gauge QCD can be identified with the running of the coupling found in Landau-DeWitt gauge within the background-field formalism. This means that we neglect possible differences between the RG flows of the fluctuation and the background field [71, 72]. The two-loop running of the coupling is indeed identical for both gauges despite the fact that the couplings are defined differently. In the deep IR, there is qualitative agreement between the Landau gauge and the Landau-DeWitt gauge indicated by the presence of a non-trivial attractive IR fixed point. This suggests a deeper connection between both gauges [33] and justifies the use of both results for the coupling for our computation of the QCD phase boundary. The differences in the results can then be considered as a measure of the influence of the gauge-field dynamics on the phase boundary.

Finally, we need to discuss how the quarks affect the running of the strong coupling. In this work, we only use a one-loop RG improved quark contribution to the gluonic anomalous dimension and therewith to the running of the strong coupling. This contribution can be straightforwardly computed from the effective action (1). Using the regulator shape functions (B4), we obtain<sup>7</sup>

$$\eta_q(\tilde{t}, \tilde{\mu}, \kappa, h) = \frac{N_f}{\sqrt{1 + \kappa h^2}} \left( 1 - \frac{1}{1 + e^{\frac{\sqrt{1 + \kappa h^2} - \tilde{\mu}}{\tilde{t}}}} - \frac{1}{1 + e^{\frac{\sqrt{1 + \kappa h^2} + \tilde{\mu}}{\tilde{t}}}} \right) \frac{4}{3} \frac{g^2}{(4\pi)^2}, \quad (62)$$

where  $m_\psi$  denotes the dimensionless quark mass, and  $\tilde{t}$  and  $\tilde{\mu}$  denote the dimensionless temperature and quark chemical potential, respectively. We recover the standard one-loop result in the limit of vanishing quark mass, chemical potential and temperature, which is as it should be. The gluonic anomalous dimension  $\eta_A$  is given by simply adding the gluonic contribution and the quark contribution:

$$\eta_F^{\text{Ref./FE}} = \eta_{\text{Ref./FE}} + \eta_q. \quad (63)$$

The running coupling of the strong coupling  $g$  including the back-reactions of the quarks is then obtained by solving the differential equation

$$\partial_t \alpha_{\text{Ref./FE}} = \eta_F^{\text{Ref./FE}} \alpha_{\text{Ref./FE}}, \quad (64)$$

which is coupled to the the RG flow equations for the Yukawa coupling  $h$  and the minimum of the scalar potential  $\kappa$ .

### III. THE PHASE BOUNDARY OF 1-FLAVOR QCD AT SMALL CHEMICAL POTENTIALS

#### A. Initial conditions and fixed-point structure of QCD

Let us now discuss our results for the phase boundary of QCD with one quark flavor. As initial conditions we use the running coupling as measured at the Z-boson mass scale  $M_Z$ ,  $\alpha_s(M_Z) \approx 0.118$  [92], and set the renormalized Yukawa coupling to  $h(M_Z) = 0.01$ , the

---

<sup>7</sup> The quark contribution  $\eta_q$  to the gluonic anomalous dimension should not be confused with the anomalous dimension associated with the quark propagator.

renormalized scalar mass to  $m^2(M_Z) \approx 5M_Z^2$  and the renormalized four-boson coupling to  $\lambda_\phi = 0$ . With this choice, the effective action at the initial scale  $M_Z$  is effectively given by

$$\Gamma_{k=M_Z} = \int d^4x \left\{ \frac{1}{4} F_{\mu\nu}^a F_{\mu\nu}^a + \bar{\psi} i \not{D} \psi \right\}. \quad (65)$$

Our choice of initial conditions is such that the results for the phase transition temperature depend only on the value of the strong coupling at the initial RG scale. The choice of the value for strong coupling at the initial scale eventually determines the absolute values of observables such as the phase transition temperature or the constituent-quark mass. Let us briefly recapitulate the results from Ref. [30] and then generalize them to the case of finite-temperature QCD.

The universal features of spontaneous chiral symmetry breaking in QCD can be nicely illustrated in terms of the fixed-point structure of the scalar couplings. This structure can be considered as the analogue of the fixed-point structure of four-fermion interactions in a purely fermionic language [31, 32]. For this purpose, we define the coupling

$$\tilde{\epsilon} = \frac{\epsilon}{h^2} = \frac{Z_\psi^2 \bar{m}^2}{k^2 h^2}. \quad (66)$$

The definition of this coupling is simply motivated by the relation  $\bar{\lambda}_\sigma \sim \bar{h}^2 / \bar{m}^2$  between the four-fermion coupling  $\bar{\lambda}_\sigma$  in the gauged NJL model and the scalar couplings  $\bar{m}^2$  and  $\bar{h}^2$  in a bosonized gauged NJL model.

The flow equation for the coupling  $\tilde{\epsilon}$  can be straightforwardly derived from the flow of the coupling  $\epsilon$  and the Yukawa coupling  $h$ . We find<sup>8</sup>

$$\begin{aligned} \beta_{\tilde{\epsilon}} \equiv \partial_t \tilde{\epsilon} = & 8N_c v_3 l_1^{\psi, (4)}(\tilde{t}, 0, \tilde{\mu}) - 8v_3 \frac{\lambda_\phi}{h^2} l_1^{B, (4)}(\tilde{t}, \epsilon) \\ & - \left( 2 - 32v_3 C_2(N_c) g^2 \left\{ L_{1,1}^{(FB), (4)}(\tilde{t}, 0, \tilde{\mu}, 0) - \frac{1}{3} \mathcal{L}_{1,1}^{(FB), (4)}(\tilde{t}, 0, \tilde{\mu}, 0) \right\} \right) \tilde{\epsilon} \\ & - 2 \left( \beta_{\lambda_\sigma}^{g^4} g^4 + \beta_{\lambda_\sigma}^{h^4} h^4 \right) \tilde{\epsilon}^2. \end{aligned} \quad (67)$$

We have neglected the anomalous dimensions for simplicity since here we are interested only in the weak coupling regime of QCD. We find that  $\beta_{\tilde{\epsilon}}$  has a UV repulsive fixed point  $\tilde{\epsilon}_1^*$  and an IR attractive fixed point  $\tilde{\epsilon}_2^*$  if the gauge coupling  $g$  is smaller than a critical value  $g_{\text{cr}}$ , see Fig. 1. For  $g = g_{\text{cr}}$ , the fixed points annihilate and the flow of  $\tilde{\epsilon}$  is not bound by any fixed

---

<sup>8</sup> Here we drop all arguments of the threshold functions associated with anomalous dimensions.



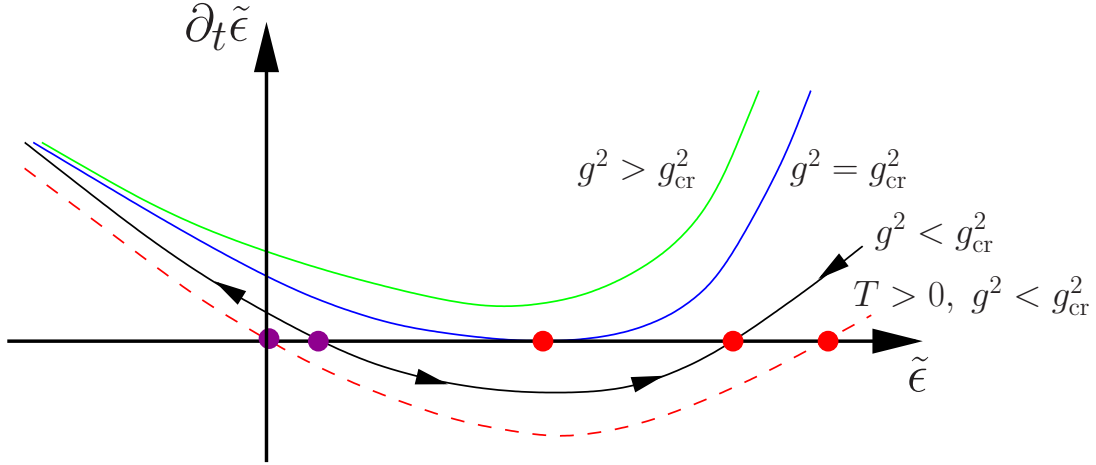


Figure 1: Sketch of the  $\beta$ -function of the coupling  $\tilde{\epsilon}$ . The figure illustrates the dependence of the flow of  $\tilde{\epsilon}$  on the gauge coupling  $g$ . The  $\beta$ -function has an UV repulsive fixed-point  $\tilde{\epsilon}_1^*$  and IR attractive fixed-point  $\tilde{\epsilon}_2^*$  if the gauge coupling  $g^2$  is smaller than a critical value  $g_{\text{cr}}^2$ . The fixed points annihilate for  $g^2 = g_{\text{cr}}^2$  and no fixed points are present for  $g^2 > g_{\text{cr}}^2$ . The red dashed line illustrates the effect of finite temperature on the result for  $g^2 < g_{\text{cr}}^2$  indicated by the black line.

points for  $g > g_{\text{cr}}$ . In the latter case, the system flows towards the regime with broken chiral symmetry characterized by a negative scalar mass parameter  $\epsilon = m^2/k^2$ . Thus,  $g > g_{\text{cr}}$  represents a necessary condition for chiral symmetry breaking and the question of whether the QCD ground-state is chirally symmetry or not has been traced back to the strength of the gauge coupling  $g$  relative to its critical value  $g_{\text{cr}}$ . We would like to mention that these considerations fully correspond to those in Refs. [31, 32, 43] where chiral symmetry breaking has been studied in terms of four-fermion interactions. The critical value of  $g_{\text{cr}}$  can be computed analytically at  $T = 0$  and  $\mu = 0$  in the limit  $\epsilon \gg 1$  from Eq. (67):

$$\alpha_{\text{cr}} = \frac{g_{\text{cr}}^2}{4\pi} \approx \frac{0.27\pi}{C_2(N_c)} \quad \implies \quad N_c g_{\text{cr}}^2 \sim \text{const. for } N_c \gg 1. \quad (68)$$

The numerical factor arises from the evaluation of the threshold functions<sup>9</sup>. Since the influence of the Yukawa coupling and the four-boson coupling can no longer be neglected near the chiral transition transition scale<sup>10</sup>, this can only serve as an estimate.

<sup>9</sup> The result for  $\alpha_{\text{cr}}$  deviates from the value in Ref. [30] due to the choice of a 3d optimized regulator-function instead of a 4d optimized regulator-function. The difference between both results is expected to be smaller in the case of finite temperature since the 4d and 3d optimized regulator function coincide in the limit  $T/k \rightarrow \infty$ .

<sup>10</sup> With respect to the influence of the scalar couplings, the estimate for  $g_{\text{cr}}$  given here does not necessarily

The fixed-point structure of the coupling  $\tilde{\epsilon}$  allows us also to divide the initial conditions into different sets. As in Ref. [30], the QCD starting point is given by  $\epsilon_\Lambda = \frac{m^2}{\Lambda^2} \gg 1$  since the scalar field is then an auxiliary field at the initial scale  $\Lambda = M_Z$  and its wave-function renormalization is tiny. Our choice for the initial conditions corresponds to a value of  $\tilde{\epsilon}$  which is close to  $\tilde{\epsilon}_2^*$ . Starting the RG flow from a set of initial conditions obeying  $\tilde{\epsilon} > \tilde{\epsilon}_2^*$  at the UV scale  $\Lambda = M_Z$ , the system flows into the fixed point  $\tilde{\epsilon}_2^*$  which then controls the evolution over a wide range of scales. This explains that the IR physics at zero temperature are not sensitive to the choice of the initial conditions [30].

At finite temperature, the situation changes slightly. For a given value of the gauge coupling  $g$ , the depth of the minimum of the  $\beta_{\tilde{\epsilon}}$ -function is increasing with an increase in the dimensionless temperature  $T/k$  and the distance between the fixed points increases, see Fig. 1. We find

$$\lim_{\tilde{t} \rightarrow \infty} \tilde{\epsilon}_2^* \rightarrow \infty. \quad (69)$$

Thus the critical value  $g_{\text{cr}}$  for the gauge coupling  $g$  increases with increasing  $T/k$  as well. This can be understood phenomenologically: The formation of a quark condensate requires stronger interactions since the quarks are thermally excited [31, 32]. In order to leave the result for the chiral phase boundary unaffected by the choice of the initial conditions, we have to choose the initial scale  $\Lambda$  in such a way that the flow is still initially governed by the fixed-point  $\tilde{\epsilon}_2^*$  given at  $T = 0$ . In practice, this can be achieved by choosing a large value for the initial scale  $\Lambda$  such that  $T/\Lambda \ll 0$  and  $\mu/\Lambda \ll 0$  for the temperatures  $T$  and quark chemical potentials  $\mu$  under consideration. Our choice  $\Lambda = M_Z$  translates into  $T/\Lambda \sim \mathcal{O}(10^{-3})$  and  $\mu/\Lambda \sim \mathcal{O}(10^{-3})$  for all of our numerical evaluations of the flow equations. Thus, our results for the phase boundary are not contaminated by the choice of the initial conditions.

Our discussion shows that the scale for all dimensionful quantities is set by the interplay between the perturbative running of the gauge coupling with its initial value, the critical value  $g_{\text{cr}}$ , and the existence of the fixed point  $\tilde{\epsilon}_2^*$ , provided we chose QCD-like initial conditions. The presence of the fixed point  $\tilde{\epsilon}_2^*$  ensures that the actual initial values for the

---

have to agree with the value found in Refs. [31, 32, 43], even if one neglects that different regulator functions have been used there. In Refs. [31, 32, 43], the authors study the influence of gluodynamics on the quark dynamics in QCD without using rebosonization techniques. The flow of the scalar couplings is then completely encoded in the RG flow of the four-fermion couplings and the estimate for  $g_{\text{cr}}$  within such a "pure" quark-gluon framework should be considered to be more accurate.

scalar couplings do not affect the absolute values for the constituent quark mass or the phase transition temperature, for example. The initial value for the gauge coupling  $g$  and its (logarithmic) running, in combination with the critical value  $g_{\text{cr}}(T/k, \mu)$ , then set a scale  $k_{\text{cr}}(T, \mu)$ . For given values of  $T$  and  $\mu$ , it is given by the solution of the equation

$$g\left(\frac{T}{k}, \frac{\mu}{k}\right) \stackrel{!}{=} g_{\text{cr}}\left(\frac{T}{k}, \frac{\mu}{k}\right). \quad (70)$$

The scale  $k_{\text{cr}}$  is naturally related to the scale  $\Lambda_{\text{QCD}}$  at which the gauge coupling becomes large. Thus the scale for all dimensionful quantities is set by  $\Lambda_{\text{QCD}}$ , independent of the initial conditions at the UV scale. Along the lines of Ref. [31, 32], one can actually use Eq. (70) to determine an upper bound for the chiral phase boundary. This is done by seeking the lowest temperature for a given  $\mu$  above which Eq. (70) does not have a solution anymore. We shall discuss this approach further in the next subsection.

Let us finally compare our approach with (P)NJL-type models. In the case of (P)NJL-type models, it is necessary to introduce a UV cutoff  $\Lambda$  which is usually on the order of 1 GeV. At this UV cutoff scale the gauge degrees of freedom are considered to be integrated out. The cutoff can therefore be considered to have a physical meaning and is needed to define the theory. The strategy is then to choose the value for the four-fermion couplings (or the scalar couplings in the context of the bosonized NJL-model, i. e. the quark-meson model) which reproduce the values of low-energy observables, such as the pion mass, the constituent-quark mass and the pion decay constant. These values of the couplings are then used to compute the chiral phase boundary in the plane of temperature and quark chemical potential. The shortcoming of this procedure is that it does not result in unique values for the initial values of the couplings at  $T = \mu = 0$ : Different sets of initial values for the couplings can reproduce the same values for the low-energy constants under consideration but lead to different predictions for the chiral phase boundary and the location of the critical point<sup>11</sup>, see e. g. Ref. [19]. If we interpret (P)NJL-type models as a low-energy formulation of QCD, we can understand their parameter ambiguity in terms of the fixed point structure of the coupling  $\tilde{e}$  by considering the limit of vanishing strong coupling  $g$ . In this limit, the

---

<sup>11</sup> Even though the predictions from Lattice QCD simulations for the curvature of the phase boundary at small chemical potentials and the location of the critical endpoint do not yet agree as well [11, 12, 19], we would like to stress that the reasons for these differences are completely different from those encountered in the context of (P)NJL-type models.

fixed-point value  $\tilde{e}_1^*$  corresponds to the value of the inverse of the critical coupling in the NJL model [29, 30]. Choosing initial conditions with  $\tilde{e}_\Lambda < \tilde{e}_1^*$ , the system is driven by strong four-fermion interactions and flows towards the regime with broken chiral symmetry. In our approach, we do not encounter such an ambiguity in the choice of the initial conditions because of the dynamically included gauge degrees of freedom and the presence of the fixed point  $\tilde{e}_2^*$ . The scale for the IR physics is uniquely fixed by our choice for the initial value of the gauge coupling  $g$  and all absolute values of the observables should be interpreted in the light of this scale-fixing procedure.

In the context of (P)NJL-type models, one might be concerned that one needs to adjust the initial values of the couplings at finite temperature. This concern is based on the observation that the temperature effects at the UV scale  $\Lambda_{\text{NJL}}$  might be non-negligible since  $T/\Lambda_{\text{NJL}} \lesssim 0.3$  for typical UV-cutoff scales  $\Lambda_{\text{NJL}}$  and temperatures used in (P)NJL-type models. As we have argued above, this problem is not present in our approach.

Despite the nice features of our RG approach, the present truncation is by no means complete, in particular with respect to additional operators which affect the mid-momentum regime where the transition to the regime with broken chiral symmetry takes place. In this regime, the flow is sensitive to higher-order operators owing to strong coupling. Examples we have in mind here are the inclusion of the Polyakov-Loop in the way proposed in a RG framework for pure Yang-Mills theory in Refs. [33, 34], or the inclusion of operators associated with instanton effects. The latter are expected to be particularly important for 1-flavor QCD. The systematic errors arising from neglecting such operators are discussed in the next subsection. In any case, we think that our approach is promising and sets the stage for future works in this direction.

## B. Results for the curvature of the phase boundary of 1-flavor QCD

Let us now discuss our numerical results for the (chiral) phase boundary of QCD with one quark flavor. As a first result, in Fig. 2 we show the temperature dependence of the quark mass for vanishing quark chemical potential. The quark mass is related to the order parameter  $\kappa$  by  $m_\psi^2 = \kappa h^2$  and tends to zero continuously for increasing temperature, which indicates a second order phase transition. This is expected since so far we have neglected  $U_A(1)$  symmetry breaking terms in our study. The results shown are obtained from the

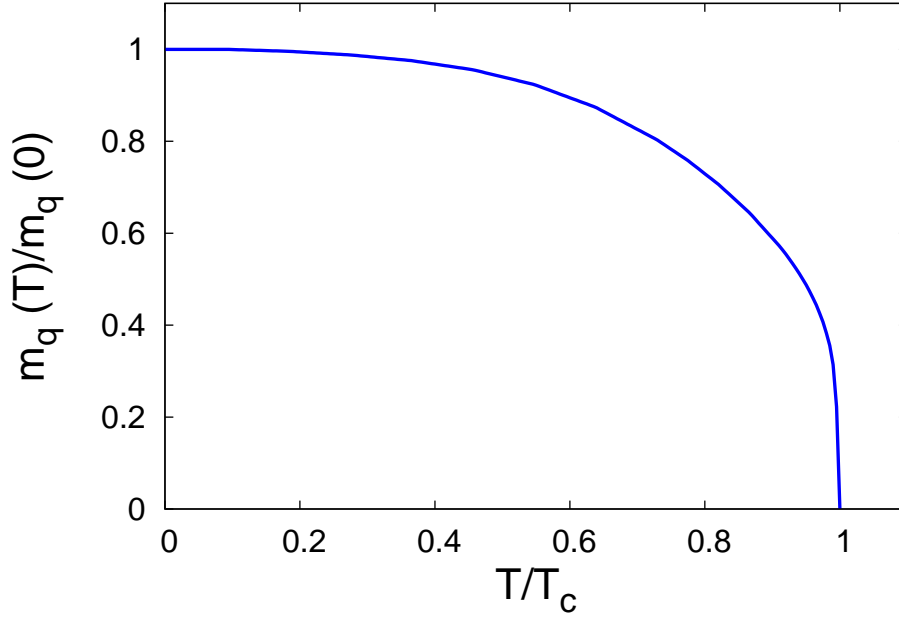


Figure 2: Temperature dependence of the quark mass for vanishing chemical potential as obtained from a calculation employing  $\alpha_{\text{Ref.}}$ . The quark mass goes continuously to zero at the critical temperature indicating a second order phase transition.

calculation employing the strong coupling  $\alpha_{\text{Ref.}}$ . For the quark mass at  $T = 0$  and  $\mu = 0$ , we find

$$m_q^{\text{Ref.}}(T = 0, \mu = 0) = 434 \text{ MeV} \quad \text{and} \quad m_q^{\text{FE}}(T = 0, \mu = 0) = 430 \text{ MeV} \quad (71)$$

for  $\alpha_{\text{Ref.}}$  and  $\alpha_{\text{FE}}$ , respectively. For  $T = 0$  and  $\mu = 0$ , the corresponding scale  $k_{\text{cr}}$  at which the RG flow enters the regime with broken chiral symmetry is given by

$$k_{\text{cr}}^{\text{Ref.}}(T = 0, \mu = 0) = 470 \text{ MeV} \quad \text{and} \quad k_{\text{cr}}^{\text{FE}}(T = 0, \mu = 0) = 330 \text{ MeV}. \quad (72)$$

For the phase transition temperature, we find

$$T_c^{\text{Ref.}}(\mu = 0) = 110 \text{ MeV} \quad \text{and} \quad T_c^{\text{FE}}(\mu = 0) = 76 \text{ MeV} \quad (73)$$

for  $\alpha_{\text{Ref.}}$  and  $\alpha_{\text{FE}}$ , respectively. The difference in the phase transition temperature is mostly due to the differences in the running of the gauge coupling in the mid-momentum regime ( $0.5 \text{ GeV} \lesssim p \lesssim 1.5 \text{ GeV}$ ). Note that the RG flow at finite temperature is less sensitive to the significant difference between the IR fixed point values of the couplings  $\alpha_{\text{Ref.}}$  and

$\alpha_{\text{FE}}$  at vanishing temperature<sup>12</sup>. This is because the RG flow of the coupling for  $k \lesssim 2\pi T$  is governed by the fixed point of the underlying  $3d$  Yang-Mills theory. Moreover, chiral symmetry breaking is triggered in the mid-momentum regime rather than in the deep IR regime. Therefore we would like to add that we expect in general that our results do not strongly depend on the behavior of the coupling in the deep IR, independent of the fact that the IR running of the strong coupling at finite temperature is governed by the underlying  $3d$  Yang-Mills theory. To be more specific, the gluons strongly influence the matter sector in the mid-momentum regime via gluon-induced four-fermion interactions. As a consequence, the gauge degrees of freedom drive the quark sector to criticality depending on the actual temperature, see Subsec. III A for details. Below the chiral symmetry breaking scale  $k_{\text{cr}}$ , the quarks acquire a finite mass. In the deep IR ( $k \sim p \lesssim 200 \text{ MeV}$ ), where currently debated differences between a scaling and a decoupling solution in the gauge sector become significant [93], the quarks are decoupled from the RG flow due to their finite mass. Therefore the influence of the gauge-sector on the (chiral) order-parameter potential (i. e. matter sector) in the deep IR is suppressed. Thus, chiral symmetry breaking is mostly sensitive to the running of the coupling in the mid-momentum regime rather than its running in the deep IR. In this respect, the findings in the present paper are in accordance with the findings in Ref. [33] where the (de-)confinement phase transition in pure SU(2)- and SU(3)-Yang-Mills theories has been studied.

As discussed in Sec. II D, we have also checked that the results are only sensitive to our ansatz for the momentum dependence of the four-fermion interaction at the percent level. Apart from these errors, systematic errors enter our calculations mainly from omitting instanton effects and deconfinement dynamics as described by the Polyakov-Loop. We expect that the transition temperature becomes larger when we include these effects. Thus the result for  $T_c$  given in Eq. (73) should be considered as a lower bound for the transition temperature. We address these issues further after the discussion of our results for the chiral phase boundary.

In order to determine the curvature of the chiral phase boundary of 1-flavor QCD at small

---

<sup>12</sup> This can be seen from looking at the ratios  $k_{\text{cr}}^{\text{FE}}(T=0, \mu=0)/k_{\text{cr}}^{\text{Ref.}}(T=0, \mu=0) \approx 0.70$  and  $T_c^{\text{FE}}(\mu=0)/T_c^{\text{Ref.}}(\mu=0) \approx 0.69$ . The almost perfect agreement of the two ratios indicates that the finite-temperature flows are less sensitive to the details of the running of the gauge coupling in the deep IR.

Author(s)	Ref.	Method	$am_c$	$N_f$	$\kappa_\mu$
J. Braun	this work	QCD RG flows	—	1	0.97 .. 1.28
J. Braun	this work	QCD RG flows: $\alpha_s$ vs. $\alpha_{cr}$	—	1	0.40 .. 0.47
P. de Forcrand et al. [2]		Lattice QCD: imag. $\mu$	0.032	2	0.500(54)
F. Karsch et al. [7]		Lattice QCD: Taylor + Rew.	0.005	3	1.13(45)
P. de Forcrand et al. [5]		Lattice QCD: imag. $\mu$	0.026	3	0.667(6)

Table I: Comparison of the results for the curvature of the QCD phase boundary for  $N_c = 3$  as obtained from Lattice QCD and QCD RG flows. The table is not exhaustive and we concentrate here on results for degenerate quark flavors with (current) mass  $am_c$ , where  $a$  denotes the lattice spacing. The RG calculations have been performed in the chiral limit. Apart from the current quark mass, the Lattice QCD simulations differ in the Lattice volumes and spacings used as well as in the implementation of the fermions.

quark chemical potential, we compute  $T_c(\mu)/T_c(0)$  for  $0 \leq \mu/T_c(0) \lesssim 0.7$ . We then extract the curvature of the phase boundary at vanishing chemical potential from these results. At small chemical potential the phase boundary can be expanded in powers of  $\mu^2$ , which yields

$$\frac{T_c(\mu)}{T_c(0)} = 1 - \kappa_\mu(N_f, N_c, m_c) \left( \frac{\mu}{\pi T_c(0)} \right)^2 + \dots \quad (74)$$

The coefficient  $\kappa_\mu$  depends on the number of quark flavors  $N_f$ , the number of colors  $N_c$  and the current quark mass. These dependences can be understood qualitatively by looking at the underlying mechanisms for chiral symmetry breaking as we discussed them in Sec. III A. The phase transition temperature and the curvature itself are sensitive to the magnitude of the quark condensate at  $T = 0$  and therefore also to the magnitude of the constituent quark mass at  $T = 0$ . The larger the constituent quark mass is for a given chemical potential  $\mu$ , the smaller is the impact of  $\mu$  on the phase transition temperature. Therefore  $\kappa_\mu$  becomes smaller with increasing (current) quark mass  $m_c$ .

The scale for the dynamically generated quark mass is essentially set by the scale  $k_{cr}$  at which the gauge coupling exceeds its critical value. The scale  $k_{cr}$  is related to the scale  $\Lambda_{QCD}$  where the gauge coupling strongly increases, thus  $k_{cr} \sim \Lambda_{QCD}$ . The flavor- and color-dependence of  $\Lambda_{QCD}$  can be estimated from the position of the Landau pole of the

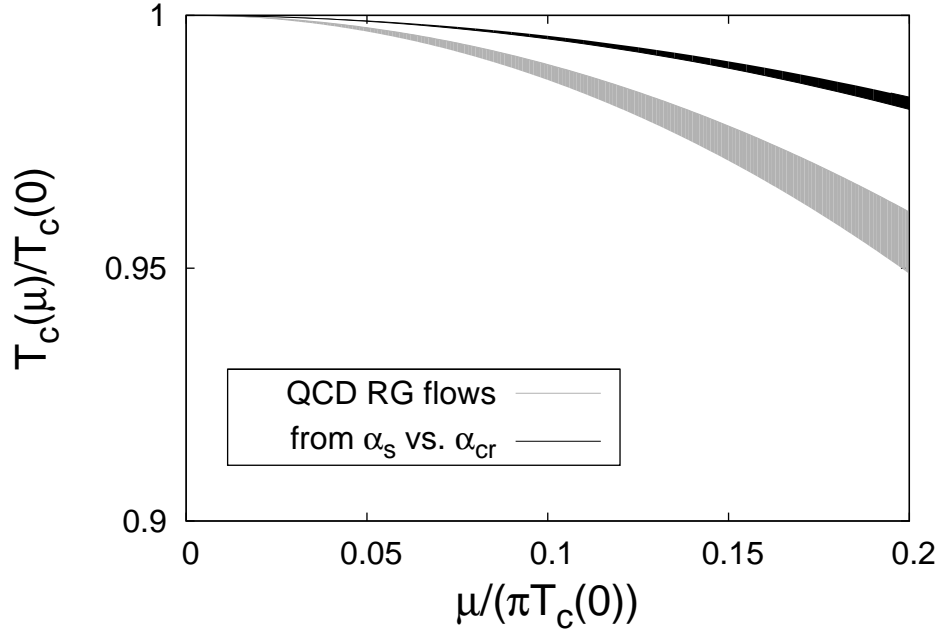


Figure 3: Phase boundary of 1-flavor QCD in terms of the dimensionless quantities  $T_{cr}(\mu)/T_{cr}(0)$  and  $\mu^2/(\pi T_{cr}(0))^2$ . The light gray band represents the results from the RG flows including the effects of gauge degrees of freedom. The black band indicates the result from an estimate of the phase boundary from a study of the running of the strong coupling  $\alpha_s$  versus  $\alpha_{cr}$  along the lines of the study in Ref. [31, 32]. The width of the bands gives the theoretical error due to uncertainties in the gauge sector.

perturbative one-loop running of the coupling<sup>13</sup> [32]:

$$\Lambda_{\text{QCD}} \sim M_Z e^{-\frac{1}{4\pi b_0 \alpha(M_Z)}} \approx M_Z e^{-\frac{6\pi}{11N_c \alpha(M_Z)}} (1 - \epsilon N_f + \mathcal{O}((\epsilon N_f)^2)) \quad (75)$$

where

$$b_0 = \frac{1}{8\pi^2} \left( \frac{11}{3} N_c - \frac{2}{3} N_f \right) \quad \text{and} \quad \epsilon = \frac{12\pi}{121 N_c^2 \alpha(M_Z)}. \quad (76)$$

We observe that  $\Lambda_{\text{QCD}}$  decreases linearly with  $N_f$ . Therefore the constituent quark mass becomes smaller with increasing  $N_f$  and  $\kappa_\mu$  bigger. For fixed  $N_f$  but increasing  $N_c$ , we find that  $\Lambda_{\text{QCD}}$  increases because  $\ln \frac{\Lambda_{\text{QCD}}}{M_Z} \sim \frac{1}{N_c}$ . Thus the quark mass increases with  $N_c$  and therefore  $\kappa_\mu$  decreases with increasing  $N_c$ . A quantitative study of the  $N_c$  dependence of

<sup>13</sup> We neglect terms arising from the chemical potential, since  $\Lambda_{\text{QCD}} \gg \mu$  for the values of the chemical potential we have in mind.



the phase boundary is work in progress [94]. We stress that these simple considerations of the dependences of the curvature in terms of the running coupling are in agreement with large  $N_c$ -considerations of the QCD phase boundary. In Ref. [95], it has been shown that  $\kappa_\mu \sim N_f/N_c$  in leading order of an expansion in powers of  $1/N_c$ .

In order to compare our results for the curvature of the phase boundary to results from lattice QCD simulations, we present our result for the phase boundary in terms of the curvature  $\kappa_\mu$ . In the first line of Tab. I and Fig. 3, we present our results for the phase boundary for QCD with one quark flavor together with results for two- and three-flavor QCD as obtained from lattice QCD simulations. We obtain

$$\kappa_\mu^{\text{Ref.}} = 0.97 \quad \text{and} \quad \kappa_\mu^{\text{FE}} = 1.28 \quad (77)$$

for  $\alpha_{\text{Ref.}}$  and  $\alpha_{\text{FE}}$ , respectively. From this, we conclude that the curvature depends significantly on the gauge-field dynamics whereas it is expected that the critical dynamics at the phase transition can be described with a simple  $O(2)$  model due to universality.

We list different lattice results for  $\kappa_\mu$  in Tab. I. From this table, we read off that the lattice result for  $\kappa_\mu$  for three degenerate quark flavors obtained with a Taylor expansion of the path integral is approximately twice as large as the result obtained with imaginary chemical potential. From our discussion above, we expect that  $\kappa_\mu$  decreases roughly linearly with decreasing  $N_f$ . Lattice QCD simulations with imaginary chemical potential are in agreement with this expectation. We compare our result for  $\kappa_\mu(N_f=1)$  with a naive linear extrapolation of  $\kappa_\mu(N_f=2)$  and  $\kappa_\mu(N_f=3)$  obtained from Lattice simulations with imaginary quark chemical potential<sup>14</sup> to  $N_f = 1$ . We then find that our result is roughly twice as large as the extrapolated value from these Lattice simulations.

Let us finally discuss the systematic errors in our results arising from neglected operators associated with instantons and quark confinement. Although our truncation allows us to study chiral symmetry breaking with its underlying mechanisms in terms of quarks and gluons, it does not yet allow us to study the deconfinement phase transition. Within the RG framework, the deconfinement phase transition in pure Yang-Mills theory with  $N_c = 2$  [33, 34], and with  $N_c = 3$  [33], has recently been successfully studied. The next step would

---

<sup>14</sup> Suitable results for  $\kappa_\mu$  obtained with sufficiently small quark masses for  $N_f = 2$  are presently not available from Lattice QCD simulations in which a Taylor expansion combined with reweighting techniques has been applied.

be to couple the RG flow of the Polyakov to the present approach. We can estimate the effects of the inclusion of the Polyakov-loop by considering Landau-DeWitt gauge,  $D_\mu(\bar{A})(\mathcal{A} - \bar{A}) = 0$ , where we identify the background field with the Polyakov-loop field,  $\bar{A} = \langle A_0 \rangle$ . The quark propagator effectively acquires an additional mass term since the vacuum expectation value of the zero-component  $\langle A_0 \rangle$  of the gauge-field shows up in the Matsubara frequencies of the quark fields as follows<sup>15</sup> [20]:

$$(\nu_n + i\mu + \bar{g}\langle A_0 \rangle)^2. \quad (78)$$

As we have discussed above, a larger quark mass translates into a flatter curvature (smaller  $\kappa_\mu$ ) and a higher (chiral) phase transition temperature, so this would be the likely effect of the Polyakov loop as well. An inclusion of the Polyakov-Loop dynamics in our RG study would eventually allow for a dynamical study of deconfinement and chiral phase transition and their interplay at the same time.

Instanton effects associated with the  $U_A(1)$  anomaly are certainly important for a more quantitative prediction of the curvature of 1-flavor QCD phase boundary since they directly influence the quark propagators. Our results for the phase boundary have been obtained from an ansatz for the effective action which has a global  $U_A(1)$  symmetry. This symmetry is broken in QCD by the presence of gauge-field configurations with non-trivial topology. Instantons are such gauge-field configurations. In the context of instantons, the  $U_A(1)$  symmetry is broken by their induction of masslike fermion interactions in 1-flavor QCD<sup>16</sup> [45, 46, 47, 48]:

$$\Gamma_{\mathcal{I}} = \int d^4x m_{\mathcal{I}} (\bar{\psi}_R \psi_L - \bar{\psi}_L \psi_R) = \int d^4x m_{\mathcal{I}} (\bar{\psi} \gamma_5 \psi). \quad (79)$$

The associated mass parameter  $m_{\mathcal{I}}$  is exponentially suppressed for small gauge coupling  $\alpha_s$ ,  $m_{\mathcal{I}}/\Lambda_{\text{QCD}} \sim e^{-2\pi/\alpha_s}$ , but becomes significantly large near the chiral transition scale, see e.g. Ref. [30]. Due to the presence of such an instanton mediated interaction, the pions acquire a mass in the deep IR as well. Therefore the instanton-mediated interactions influence directly the curvature of the phase boundary and the phase transition temperature. Since the instanton-mediated interactions act like an explicit mass term for the quark fields, we

<sup>15</sup> We have  $\langle A_0 \rangle = 0$  only for  $T \rightarrow \infty$ .

<sup>16</sup> The treatment of instantons within the functional RG framework has been discussed in detail in Refs. [30, 96].

expect the curvature to become flatter, the phase transition temperature to become higher and the second order phase transition to turn into a crossover.

Although we do not study the effects of a broken global  $U_A(1)$  symmetry and an inclusion of the Polyakov-Loop dynamics explicitly, we can give an estimate how they affect the phase boundary by using Eq. (70) to determine the phase boundary. Estimating the phase boundary from Eq. (70) means to effectively stop the RG flow at the scale  $k_{\text{cr}}$  at which the strong coupling exceeds its critical value. We find  $k_{\text{cr}} \approx 1.5 \text{ GeV}$  for  $\alpha_{\text{Ref.}}$  and  $k_{\text{cr}} \approx 0.9 \text{ GeV}$  for  $\alpha_{\text{FE}}$ . Our results for the curvature  $\kappa_\mu$  are given in Tab. I. We find that the estimated values for  $\kappa_\mu$  are

$$\kappa_\mu^{\text{Ref.}} = 0.47 \quad \text{and} \quad \kappa_\mu^{\text{FE}} = 0.40, \quad (80)$$

which are smaller by roughly a factor of two compared to those values obtained from a solution of the full set of flow equations, see Eq. (77) and Tab. I. This is due to the fact that the massless Goldstone modes dominating the IR physics are effectively cut off when we estimate the phase boundary from Eq. (70). Instanton-mediated fermionic interactions effectively introduce an IR cutoff for both the fermions and the bosons in the IR which is roughly of the order of 1 GeV in case of 1-flavor QCD [30]. Therefore our estimate of the curvature of the phase boundary from Eq. (70) is less contaminated by these topological aspects of QCD and serve as an estimate for a lower bound for the curvature  $\kappa_\mu$ . A quantitative analysis of the influence of topological effects on the QCD phase boundary is postponed to future work [97]. Moreover we observe that the uncertainty for the curvature in Eq. (80), obtained from our estimate for the critical gauge coupling, is much smaller than the uncertainty found in the results from a solution of the full set of RG flow equations, see Eq. (77). This is due to the fact that the running coupling exceeds its critical value on scales where its running is still close to the perturbative 2-loop running and the differences between  $\alpha_{\text{Ref.}}$  and  $\alpha_{\text{FE}}$  are therefore small. On the other hand the results (77) for the curvature from the solution of the full set of RG flow equations are sensitive to the non-perturbative running of the gauge coupling in the mid-momentum regime ( $p \sim 0.5 - 1 \text{ GeV}$ ). Therefore the uncertainty in the curvature  $\kappa_\mu$  reflects mostly the uncertainty in our truncation of the gauge sector.

#### IV. SUMMARY AND CONCLUSIONS

In this paper we have presented a functional RG approach which allows to study the QCD phase boundary from first principles. Our work aims to set the stage for future studies in this direction incorporating two and three quark flavors. As a first application, we have computed the phase boundary of 1-flavor QCD at small chemical potential and found a second order phase transition if  $U_A(1)$  violating terms are neglected. However, our study in its present form does not allow us to detect a critical endpoint in the phase diagram of 1-flavor QCD since it relies on a low-order expansion in  $n$ -point functions in the scalar sector with  $n \leq 4$ . Therefore the reliability (i. e. the radius of convergence) of a Taylor expansion of the chiral phase boundary in powers of the quark chemical potential cannot be checked. With respect to the nature of the phase transition, however, we expect our truncation to be reliable for small chemical potentials (at least for  $\mu = 0$ ). In this regime the nature of the finite-temperature phase transition is dominated by the underlying  $O(2)$  symmetry while quark effects are subleading<sup>17</sup>. An improvement of our truncation with respect to an inclusion of higher  $n$ -point functions in the scalar sector of our truncation, which allows us to search for a critical endpoint, is deferred to future work.

Apart from a numerical study of the phase boundary, we have discussed the underlying mechanisms of chiral symmetry breaking in terms of quark-gluon dynamics and how these mechanisms relate to the dependence of the curvature on the number of quark flavors  $N_f$ , the number of colors  $N_c$  and the current quark mass  $m_c$ . In particular, we have argued that the curvature is linearly dependent on  $N_f/N_c$ .

Although the present approach contains already all ingredients that are necessary for a study of the QCD phase diagram from first principles, our numerical predictions for the phase boundary at small chemical potentials suffer from the underlying approximations. As we have already discussed above, our present low-order expansion of the scalar sector in terms of  $n$ -point functions does not allow us to detect a first-order phase transition. Moreover, we have further theoretical errors entering our study due to our truncation of the gauge sector. In order to "measure" the uncertainties arising from this sector we have used the running gauge coupling from a functional RG study employing the background-

---

<sup>17</sup> Even though gluon-induced quark interactions drive the system towards the phase transition, quark effects can be suppressed at the phase transition.

field method [31, 32] and from lattice QCD [77] as an input. Thereby we have exploited the fact that the coupling of the gauge sector and the matter sector is dominantly given by the running gauge coupling, the wave-function renormalizations of the gluons as well as the quark mass. We found that the curvature of the phase boundary is about 30% smaller for the lattice coupling than for the background-field coupling. This suggests that the curvature of the phase boundary is indeed sensitive to the underlying gauge-field dynamics beyond large  $N_c$  which is an important result for presently used (P)NJL-type models. With respect to the current debate on scaling versus decoupling scenario in the gauge sector, see e. g. Ref. [93], our analysis suggests that the behavior of the propagators in the deep IR does not strongly influence the shape of the phase boundary. This observation is in accordance with a study of the deconfinement phase transition in pure Yang-Mills theory [33].

Apart from our analysis of the role of the gauge-field dynamics essentially stemming from the gluonic two-point function, we have an uncertainty originating from the fact that we have expanded the gauge-sector about a vanishing  $\langle A_0 \rangle$  instead of taking its temperature and scale-dependence into account [33]. Concerning  $U_A(1)$ -violating terms, we have provided an estimate of their influence on the phase boundary. We have argued that we expect the curvature of the QCD phase diagram at small chemical potentials to become flatter by a factor of two when these two missing pieces are included. This leads us to an estimate for a lower bound for the curvature of the phase boundary. We add that this estimate for the curvature compares nicely with a linear extrapolation to  $N_f = 1$  of lattice QCD studies for  $N_f = 2, 3, 4$  with imaginary chemical potential, see Refs. [2, 3, 4, 5]. Finally we would like to mention that instanton effects as well as an expansion of the gauge sector about a scale and temperature-dependent  $\langle A_0 \rangle$  can be included dynamically in our study by combining it with the findings in Refs. [96] and [33], respectively.

We conclude that our approach allows us to compute the phase boundary unambiguously in the sense that the scale for all of our results is set by a single input parameter, namely the value of the strong coupling  $\alpha_s$  at e. g. the Z-boson mass scale. This is a great advantage compared to studies of the QCD phase diagram in terms of (P)NJL-type models, in which the results for the curvature and the location of a (possible) critical endpoint in the phase diagram strongly depend on the choice of the UV cutoff and a set of input parameters. Therefore we think that the present approach is very promising since it allows to bridge the gap between quarks and gluons on the one hand and hadronic degrees of freedom on the

other and opens up the possibility of studies of the QCD phase diagram with two and three quark flavors which depend on only a single physical input parameter.

### Acknowledgments

The author is deeply indebted to Holger Gies, Bertram Klein and Jan Martin Pawłowski for many helpful and enlightening discussions and useful comments on the manuscript. The author is also grateful to Ian Allison and Philippe de Forcrand for very useful discussions. This work was supported by the Natural Sciences and Engineering Research Council of Canada (NSERC). TRIUMF receives federal funding via a contribution agreement through the National Research Council of Canada.

### Appendix A: DEFINITION OF THE PROPAGATORS

We define the boson propagator as follows:

$$P_B(p_0, \{p_i\}) = \frac{1}{Z_B^\parallel(p_0, \{p_i\})p_0^2 + Z_B^\perp(p_0, \{p_i\})\vec{p}^2(1 + r_B) + M_B^2}. \quad (\text{A1})$$

For the fermions, it is convenient to define the modified four-momenta:

$$\not{p}^{(\mp)} = \mp \gamma_\mu \cdot \left( \frac{Z_\psi^\parallel(\mp p_0, \{\mp p_i\})}{Z_\psi^\perp(\mp p_0, \{\mp p_i\})} \frac{\mp p_0 + i\mu}{1 + r_\psi}, \mp p_i \right) \equiv \mp \gamma_\mu \cdot \tilde{p}_\mu^{(\pm)}. \quad (\text{A2})$$

The fermion propagator can then be written as

$$P_\psi^{(+)}(M_\psi) = \mathcal{P}^{(+)}(M_\psi) [\not{p}^{(+)} - (1 + r_\psi)^{-1} M_\psi], \quad (\text{A3})$$

$$P_\psi^{(-)}(M_\psi) = \mathcal{P}^{(-)}(M_\psi) [\not{p}^{(-)} + (1 + r_\psi)^{-1} M_\psi] \quad (\text{A4})$$

with

$$\begin{aligned} \mathcal{P}^{(\mp)}(M_\psi) \\ = \frac{-Z_\psi^\perp(\mp p_0, \{\mp p_i\})(1 + r_\psi)}{(Z_\psi^\parallel(\mp p_0, \{\mp p_i\})(\mp p_0 + i\mu))^2 + (Z_\psi^\perp(\mp p_0, \{\mp p_i\})\vec{p}(1 + r_\psi))^2 + M_\psi^2}. \end{aligned} \quad (\text{A5})$$

We should keep in mind that  $M_\psi$  is in general a complicated function depending on the background fields, the Yukawa coupling, the gauge coupling as well as the four-momentum<sup>18</sup>:

$$M_\psi \equiv M_\psi(p_0, \{p_i\}, \{\Phi_i\}, h, g, \{\bar{A}_\mu\}), \quad (\text{A6})$$

---

<sup>18</sup> Note that the couplings depend in general on the momenta as well.

where  $\Phi$  represents a two-dimensional vector of real scalar fields.

Finally, the gauge-field propagator is given by

$$P_A(p_0, \{p_i\}) = \frac{1}{Z_F^\parallel(p_0, \{p_i\})p_0^2 + Z_F^\perp(p_0, \{p_i\})\vec{p}^2(1 + r_B)} \left( \delta_{\mu\nu} - \frac{p_\mu p_\nu}{p^2} \right) + \frac{\xi}{p_0^2 + \vec{p}^2(1 + r_B)} \left( \frac{p_\mu p_\nu}{p^2} \right), \quad (\text{A7})$$

where  $\xi$  is the gauge-fixing parameter.

## Appendix B: THRESHOLD FUNCTIONS

The regulator dependence of the flow equations is controlled by (dimensionless) threshold functions which arise from Feynman graphs, incorporating fermionic and/or bosonic elds. Let us first introduce the so-called dimensionless regulator-shape function  $r_B(x)$  and  $r_\psi(x)$  for bosonic and fermionic fields. These functions are implicitly defined by the regulator function  $R_i$  as follows:

$$R_B(p_0, \{p_i\}) = Z_{B,k}^\perp(p_0, \{p_i\})\vec{p}^2 r_B(\vec{p}^2/k^2) \quad (\text{B1})$$

for the bosonic fields and

$$R_\psi(p_0, \{p_i\}) = Z_{\psi,k}^\perp(p_0, \{p_i\})\not{\vec{p}} r_\psi(\vec{p}^2/k^2) \quad (\text{B2})$$

for the fermionic fields. For the gauge fields, we choose

$$R_A(p_0, \{p_i\}) = Z_{F,k}^\perp(p_0, \{p_i\})\vec{p}^2 r_B(\vec{p}^2/k^2) \left( \delta_{\mu\nu} - \frac{p_\mu p_\nu}{p^2} \right) + \frac{1}{\xi} \vec{p}^2 r_B(\vec{p}^2/k^2) \left( \frac{p_\mu p_\nu}{p^2} \right). \quad (\text{B3})$$

In this work, we employ a  $3d$  optimized regulator-shape function [23, 51, 52]:

$$r_B(x) = \left( \frac{1}{x} - 1 \right) \Theta(1 - x) \quad \text{and} \quad r_\psi = \left( \frac{1}{\sqrt{x}} - 1 \right) \Theta(1 - x). \quad (\text{B4})$$

In the following, we use these regulator shape functions whenever we evaluate the integrals and sums in our general definitions of the threshold functions.

In order to define the threshold functions, it is convenient to define dimensionless propagators for the scalars (B), gluons (A) and fermions ( $\psi$ ), respectively:

$$\tilde{G}_{B,A}(x_0, \omega) = \frac{1}{z_{B,A}x_0 + x(1 + r_B) + \omega} \quad (\text{B5})$$

and

$$\tilde{G}_\psi(x_0, \omega) = \frac{1}{z_\psi^2 x_0 + x(1 + r_\psi)^2 + \omega}, \quad (\text{B6})$$

where  $z_B = Z_B^\parallel/Z_B^\perp$ ,  $z_A = Z_F^\parallel/Z_F^\perp$  and  $z_\psi = Z_\psi^\parallel/Z_\psi^\perp$  give the ratio of the wave-function renormalization in the direction parallel and perpendicular to the heat-bath.

First, we define the threshold functions which encounter in the flow equations for the effective potential. For the bosonic loops, we find

$$\begin{aligned} l_0^{(B),(d)}(\tilde{t}, \omega; \eta_B) &= \frac{\tilde{t}}{2} \sum_{n=-\infty}^{\infty} \int_0^\infty dx x^{\frac{d-1}{2}} (\partial_t r_B - \eta_B r_B) \tilde{G}_B(\tilde{\omega}_n^2, \omega) \\ &= \frac{2}{d-1} \frac{1}{\sqrt{1+\omega}} \left(1 - \frac{\eta_B}{d+1}\right) \left(\frac{1}{2} + \bar{n}_B(\tilde{t}, \omega)\right) \end{aligned} \quad (\text{B7})$$

where  $\tilde{t} = T/k$  denotes the dimensionless temperature and  $\tilde{\omega} = 2\pi n\tilde{t}$  denotes the dimensionless bosonic Matsubara frequencies. The function  $n_B$  represents the Bose-Einstein distribution function

$$\bar{n}_B(\tilde{t}, \omega) = \frac{1}{e^{\sqrt{1+\omega}/\tilde{t}} - 1}. \quad (\text{B8})$$

Bosonic threshold functions of order  $n$  are then derived from Eq. (B7) by induction:

$$\frac{\partial}{\partial \omega} l_n^{(B),(d)}(\tilde{t}, \omega; \eta_B) = -(n + \delta_{n,0}) l_{n+1}^{(B),(d)}(\tilde{t}, \omega; \eta_B). \quad (\text{B9})$$

For the fermion loops contributing to the flow equations of the effective potential, we find

$$\begin{aligned} l_0^{(F),(d)}(\tilde{t}, \omega, \tilde{\mu}; \eta_\psi) &= \tilde{t} \sum_{n=-\infty}^{\infty} \int_0^\infty dx x^{\frac{d-1}{2}} (\partial_t r_\psi - \eta_\psi r_\psi) (1 + r_\psi) \tilde{G}_\psi((\tilde{\nu}_n + i\tilde{\mu})^2, \omega) \\ &= \frac{1}{d-1} \frac{1}{\sqrt{1+\omega}} \left(1 - \frac{\eta_\psi}{d}\right) (1 - \bar{n}_\psi(\tilde{t}, \tilde{\mu}, \omega) - \bar{n}_\psi(\tilde{t}, -\tilde{\mu}, \omega)). \end{aligned} \quad (\text{B10})$$

Here, we have introduced the dimensionless fermionic Matsubara frequencies  $\tilde{\nu}_n = (2n+1)\pi\tilde{t}$ , the dimensionless chemical potential  $\tilde{\mu} = \mu/k$  and the Fermi-Dirac distribution functions  $n_\psi$ :

$$\bar{n}_\psi(\tilde{t}, \tilde{\mu}, \omega) = \frac{1}{e^{(\sqrt{1+\omega}-\tilde{\mu})/\tilde{t}} + 1} \xrightarrow{\tilde{t} \rightarrow 0} \Theta(\tilde{\mu} - \sqrt{1+\omega}). \quad (\text{B11})$$

Higher-order fermionic threshold functions are also given by induction:

$$\frac{\partial}{\partial \omega} l_n^{(F),(d)}(\tilde{t}, \omega, \tilde{\mu}; \eta_\psi) = -(n + \delta_{n,0}) l_{n+1}^{(F),(d)}(\tilde{t}, \omega, \tilde{\mu}; \eta_\psi). \quad (\text{B12})$$



Let us now define the threshold functions which are involved in the computation of the Yukawa coupling. We have

$$L_{1,1}^{(FB),(d)}(\tilde{t}, \omega_\psi, \tilde{\mu}, \omega_B, \tilde{Q}_0; \eta_\psi, \eta_B) = -\frac{\tilde{t}}{2} \sum_{n=-\infty}^{\infty} \int_0^\infty dx x^{\frac{d-3}{2}} \tilde{\partial}_t \tilde{G}_\psi((\tilde{\nu}_n + i\tilde{\mu})^2, \omega_\psi) \tilde{G}_B((\tilde{\nu}_n - \tilde{Q}_0)^2, \omega_B). \quad (\text{B13})$$

In order to evaluate the integral over  $x$  (spatial momenta), we use<sup>19</sup>

$$\tilde{\partial}_t \Big|_\psi = \left( \frac{1}{x^{1/2}} - \eta_\psi \left( \frac{1}{x^{1/2}} - 1 \right) \right) \Theta(1-x) \frac{\partial}{\partial r_\psi}, \quad (\text{B14})$$

$$\tilde{\partial}_t \Big|_B = \left( \frac{2}{x} - \eta_B \left( \frac{1}{x} - 1 \right) \right) \Theta(1-x) \frac{\partial}{\partial r_\psi}, \quad (\text{B15})$$

$$(\text{B16})$$

where the first and the second line tells us how the formal derivative  $\tilde{\partial}_t$  acts on fermions and bosons, respectively. The threshold function  $L_{1,1}^{(FB),(d)}$  reads then

$$L_{1,1}^{(FB),(d)}(\tilde{t}, \omega_\psi, \tilde{\mu}, \omega_B, \tilde{Q}_0; \eta_\psi, \eta_B) = \frac{2\tilde{t}}{d-1} \sum_{n=-\infty}^{\infty} \mathcal{G}_\psi((\tilde{\nu}_n + i\tilde{\mu})^2, \omega_\psi) \mathcal{G}_B((\tilde{\nu}_n - \tilde{Q}_0)^2, \omega_B) \left\{ \left( 1 - \frac{\eta_\psi}{d} \right) \mathcal{G}_\psi((\tilde{\nu}_n + i\tilde{\mu})^2, \omega_\psi) + \left( 1 - \frac{\eta_B}{d+1} \right) \mathcal{G}_B((\tilde{\nu}_n - \tilde{Q}_0)^2, \omega_B) \right\}, \quad (\text{B17})$$

where we have introduced the auxiliary functions

$$\mathcal{G}_\psi(x_0, \omega) = \frac{1}{z_\psi x_0 + 1 + \omega}, \quad (\text{B18})$$

$$\mathcal{G}_B(x_0, \omega) = \frac{1}{z_B x_0 + 1 + \omega}. \quad (\text{B19})$$

In Landau gauge (or any other gauge with gauge-fixing parameter  $\xi \neq 1$ ), we encounter additional threshold functions in the flow equations for the Yukawa coupling due to the

---

<sup>19</sup> Here, we give only explicit expressions for the formal derivatives obtained with the regulator shape functions (B4).

presence of longitudinal gauge bosons:

$$\begin{aligned}
& \mathcal{L}_{1,1}^{(FB),(d)}(\tilde{t}, \omega_\psi, \tilde{\mu}, \omega_B, \tilde{Q}_0; \eta_\psi, \eta_B) \\
&= -\frac{\tilde{t}}{2} \sum_{n=-\infty}^{\infty} \int_0^{\infty} dx \frac{x^{\frac{d-1}{2}}}{(\tilde{\nu}_n - \tilde{Q}_0)^2 + x} \tilde{\partial}_t \tilde{G}_\psi((\tilde{\nu}_n + i\tilde{\mu})^2, \omega_\psi) \tilde{G}_B((\tilde{\nu}_n - \tilde{Q}_0)^2, \omega_B) \\
&= \tilde{t} \sum_{n=-\infty}^{\infty} \mathcal{G}_\psi((\tilde{\nu}_n + i\tilde{\mu})^2, \omega_\psi) \mathcal{G}_B((\tilde{\nu}_n - \tilde{Q}_0)^2, \omega_B) \left\{ \left( H_{(d-1)}^{(1)}((\tilde{\nu}_n - \tilde{Q}_0)^2) \right. \right. \\
&\quad \left. \left. - \eta_\psi \left( H_{(d-1)}^{(1)}((\tilde{\nu}_n - \tilde{Q}_0)^2) - H_d^{(1)}((\tilde{\nu}_n - \tilde{Q}_0)^2) \right) \right) \mathcal{G}_\psi((\tilde{\nu}_n + i\tilde{\mu})^2, \omega_\psi) \right. \\
&\quad \left. + \left( H_{(d-1)}^{(1)}((\tilde{\nu}_n - \tilde{Q}_0)^2) - \frac{\eta_B}{2} \left( H_{(d-1)}^{(1)}((\tilde{\nu}_n - \tilde{Q}_0)^2) \right. \right. \right. \\
&\quad \left. \left. \left. - H_{(d+1)}^{(1)}((\tilde{\nu}_n - \tilde{Q}_0)^2) \right) \right) \mathcal{G}_B((\tilde{\nu}_n - \tilde{Q}_0)^2, \omega_B) \right\}, \tag{B20}
\end{aligned}$$

where the auxiliary functions  $H_d(z)$  are given by<sup>20</sup>

$$H_d^{(m)}(z) = \int_0^1 dx \left( \frac{x^{d/2}}{z+x} \right)^m. \tag{B21}$$

Next, we discuss the threshold functions which are involved in the computation of the wave-function renormalizations. We shall start with the threshold functions for the fermionic wave-function  $Z_\psi$  renormalization due to its close relation to those for the Yukawa coupling. Overall, we have three different types of threshold-functions contributing to the flow of  $Z_\psi$ . The first one is closely related to those functions found in Refs. [30, 62] and reads:

$$\begin{aligned}
& \mathcal{M}_{1,2}^{(FB),(d)}(\tilde{t}, \omega_\psi, \tilde{\mu}, \omega_B, \tilde{Q}_0; \eta_\psi, \eta_B) \\
&= \frac{\tilde{t}}{2} \sum_{n=-\infty}^{\infty} \int_0^{\infty} dx x^{\frac{d-1}{2}} \tilde{\partial}_t \left\{ (1 + r_\psi) \tilde{G}_\psi((\tilde{\nu}_n + i\tilde{\mu})^2, \omega_\psi) \frac{d}{dx} \tilde{G}_B((\tilde{\nu}_n - \tilde{Q}_0)^2, \omega_B) \right\}. \tag{B22}
\end{aligned}$$

Evaluating the integration over  $x$ , we find

$$\begin{aligned}
& \mathcal{M}_{1,2}^{(FB),(d)}(\tilde{t}, \omega_\psi, \tilde{\mu}, \omega_B, \tilde{Q}_0) \\
&= \left( 1 - \frac{\eta_B}{d} \right) \tilde{t} \sum_{n=-\infty}^{\infty} \mathcal{G}_\psi((\tilde{\nu}_n + i\tilde{\mu})^2, \omega_\psi) \left( \mathcal{G}_B((\tilde{\nu}_n - \tilde{Q}_0)^2, \omega_B) \right)^2. \tag{B23}
\end{aligned}$$

Due to our choice of the regulator functions,  $\mathcal{M}_{1,2}^{(FB),(d)}$  is independent of  $Z_\psi$ , even for  $\partial_t Z_\psi \neq 0$ . The second type of threshold function that we encounter is given by

$$\begin{aligned}
& \mathcal{N}_{1,2}^{(FB),(d)}(\tilde{t}, \omega_\psi, \tilde{\mu}, \omega_B, \tilde{Q}_0; \eta_\psi, \eta_B) \\
&= \frac{\tilde{t}}{2} \sum_{n=-\infty}^{\infty} \int_0^{\infty} dx \frac{x^{\frac{d-1}{2}+1}}{(\tilde{\nu}_n - \tilde{Q}_0)^2 + x} \tilde{\partial}_t \left\{ (1 + r_\psi) \tilde{G}_\psi((\tilde{\nu}_n + i\tilde{\mu})^2, \omega_\psi) \frac{d}{dx} \tilde{G}_B((\tilde{\nu}_n - \tilde{Q}_0)^2, \omega_B) \right\}. \tag{B24}
\end{aligned}$$

<sup>20</sup> The functions  $H_d(z)$  are related to the Hypergeometric function  ${}_2F_1$ , see e. g. [98].

As in the case of the threshold functions for the flow of the Yukawa-coupling, this threshold function as well as the next threshold function that we are going to discuss is only present in gauges with gauge-fixing parameter  $\xi \neq 1$ . Due to the similar momentum structure of  $\mathcal{N}_{1,2}^{(FB),(d)}$  and  $\mathcal{M}_{1,2}^{(FB),(d)}$ , we immediately obtain

$$\begin{aligned} \mathcal{N}_{1,2}^{(FB),(d)}(\tilde{t}, \omega_\psi, \tilde{\mu}, \omega_B, \tilde{Q}_0; \eta_\psi, \eta_B) \\ = \tilde{t} \sum_{n=-\infty}^{\infty} \mathcal{G}_\psi((\tilde{\nu}_n + i\tilde{\mu})^2, \omega_\psi) \left( \mathcal{G}_B((\tilde{\nu}_n - \tilde{Q}_0)^2, \omega_B) \right)^2 \left( \frac{1}{1 + (\tilde{\nu}_n - \tilde{Q}_0)^2} \right. \\ \left. - \frac{\eta_B}{2} H_d^{(1)}((\tilde{\nu}_n - \tilde{Q}_0)^2) \right) \end{aligned} \quad (\text{B25})$$

for the given choice of the regulator functions. The last threshold functions present in the RG flows of  $Z_\psi$  is a generalization of an already know threshold function found in Ref. [30]:

$$\begin{aligned} \tilde{\mathcal{N}}_{1,1,m}^{(FB),(d)}(\tilde{t}, \omega_\psi, \tilde{\mu}, \omega_B, \tilde{Q}_0; \eta_\psi, \eta_B) \\ = -\frac{\tilde{t}}{2} \sum_{n=-\infty}^{\infty} \int_0^\infty dx \frac{x^{\frac{d-3}{2}+m}}{((\tilde{\nu}_n - \tilde{Q}_0)^2 + x)^m} \tilde{\partial}_t \left\{ (1 + r_\psi) \tilde{G}_\psi((\tilde{\nu}_n + i\tilde{\mu})^2, \omega_\psi) \tilde{G}_B((\tilde{\nu}_n - \tilde{Q}_0)^2, \omega_B) \right\}. \end{aligned} \quad (\text{B26})$$

The integral over  $x$  can be performed straightforwardly, yielding

$$\begin{aligned} \tilde{\mathcal{N}}_{1,1,m}^{(FB),(d)}(\tilde{t}, \omega_\psi, \tilde{\mu}, \omega_B, \tilde{Q}_0; \eta_\psi, \eta_B) \\ = -\frac{\tilde{t}}{2} \sum_{n=-\infty}^{\infty} \mathcal{G}_\psi((\tilde{\nu}_n + i\tilde{\mu})^2, \omega_\psi) \mathcal{G}_B((\tilde{\nu}_n - \tilde{Q}_0)^2, \omega_B) \left\{ H_{(d-4)}^{(m)}((\tilde{\nu}_n - \tilde{Q}_0)^2) \right. \\ - \eta_\psi \left[ H_{(d-4)}^{(m)}((\tilde{\nu}_n - \tilde{Q}_0)^2) - H_{(d-3)}^{(m)}((\tilde{\nu}_n - \tilde{Q}_0)^2) \right] - 2\mathcal{G}_\psi((\tilde{\nu}_n + i\tilde{\mu})^2, \omega_\psi) H_{(d-4)}^{(m)}((\tilde{\nu}_n - \tilde{Q}_0)^2) \\ + 2\eta_\psi \mathcal{G}_\psi((\tilde{\nu}_n + i\tilde{\mu})^2, \omega_\psi) \left[ H_{(d-4)}^{(m)}((\tilde{\nu}_n - \tilde{Q}_0)^2) - H_{(d-3)}^{(m)}((\tilde{\nu}_n - \tilde{Q}_0)^2) \right] \\ - 2\mathcal{G}_B((\tilde{\nu}_n - \tilde{Q}_0)^2, \omega_B) H_{(d-4)}^{(m)}((\tilde{\nu}_n - \tilde{Q}_0)^2) + \eta_B \mathcal{G}_B((\tilde{\nu}_n - \tilde{Q}_0)^2, \omega_B) \left[ H_{(d-4)}^{(m)}((\tilde{\nu}_n - \tilde{Q}_0)^2) \right. \\ \left. \left. - H_{(d-2)}^{(m)}((\tilde{\nu}_n - \tilde{Q}_0)^2) \right] \right\}. \end{aligned} \quad (\text{B27})$$

The threshold functions needed for the computation of the scalar anomalous dimensions are given by

$$\mathcal{M}_{2,2}^{(B),(d)}(\tilde{t}, \omega_1, \omega_2; \eta_B) = -\frac{\tilde{t}}{2} \sum_{n=-\infty}^{\infty} \int_0^\infty dx x^{\frac{d-1}{2}} \tilde{\partial}_t \left( \frac{d}{dx} \tilde{G}_B(\tilde{\omega}_n^2, \omega_1) \right) \left( \frac{d}{dx} \tilde{G}_B(\tilde{\omega}_n^2, \omega_2) \right). \quad (\text{B28})$$

The integration over  $x$  can be performed analytically for the regulator shape functions under consideration and we obtain

$$\mathcal{M}_{2,2}^{(B),(d)}(\tilde{t}, \omega_1, \omega_2; \eta_B) = \tilde{t} \sum_{n=-\infty}^{\infty} \left( \mathcal{G}_B(\tilde{\omega}_n^2, \omega_1) \right)^2 \left( \mathcal{G}_B(\tilde{\omega}_n^2, \omega_2) \right)^2. \quad (\text{B29})$$

Note that  $\mathcal{M}_{2,2}^{(B),(d)}$  is independent of  $\eta_\phi$  for our choice of the regulator functions as it has already been found in Ref. [99]. Two more contributions to the scalar anomalous dimensions come from purely fermionic loops. One of those contributions is proportional to the square of the vacuum expectation value of the scalar field and the corresponding threshold function reads

$$\mathcal{M}_2^{(F),(d)}(\tilde{t}, \omega, \tilde{\mu}; \eta_\psi) = -\frac{\tilde{t}}{2} \sum_{n=-\infty}^{\infty} \int_0^\infty dx x^{\frac{d-1}{2}} \tilde{\partial}_t \left( \frac{d}{dx} \tilde{G}_\psi((\tilde{\nu}_n + i\tilde{\mu})^2, \omega) \right)^2. \quad (\text{B30})$$

The integration over  $x$  can be carried out analytically and we find again that  $\mathcal{M}_{2,2}^{(F),(d)}$  is independent of the fermionic anomalous dimensions for the cutoff function under consideration:

$$\mathcal{M}_2^{(F),(d)}(\tilde{t}, \omega, \tilde{\mu}; \eta_\psi) = \tilde{t} \sum_{n=-\infty}^{\infty} (\mathcal{G}_\psi((\tilde{\nu}_n + i\tilde{\mu})^2, \omega))^4. \quad (\text{B31})$$

The threshold function of the second contribution consisting solely of fermionic internal lines is given by

$$\mathcal{M}_4^{(F),(d)}(\tilde{t}, \omega, \tilde{\mu}; \eta_\psi) = -\frac{\tilde{t}}{2} \sum_{n=-\infty}^{\infty} \int_0^\infty dx x^{\frac{d+1}{2}} \tilde{\partial}_t \left( \frac{d}{dx} (1 + r_\psi) \tilde{G}_\psi((\tilde{\nu}_n + i\tilde{\mu})^2, \omega) \right)^2. \quad (\text{B32})$$

Performing the integration over  $x$ , we find

$$\begin{aligned} \mathcal{M}_4^{(F),(d)}(\tilde{t}, \omega, \tilde{\mu}; \eta_\psi) = \tilde{t} \sum_{n=-\infty}^{\infty} \left\{ (\mathcal{G}_\psi((\tilde{\nu}_n + i\tilde{\mu})^2, \omega))^4 + \frac{1 - \eta_\psi}{d - 3} (\mathcal{G}_\psi((\tilde{\nu}_n + i\tilde{\mu})^2, \omega))^3 \right. \\ \left. - \left( \frac{1 - \eta_\psi}{2d - 6} + \frac{1}{4} \right) (\mathcal{G}_\psi((\tilde{\nu}_n + i\tilde{\mu})^2, \omega))^2 \right\}. \quad (\text{B33}) \end{aligned}$$

Finally, we have to discuss the threshold functions corresponding to 1 PI box diagrams. These threshold functions are needed for a computation of the RG flow of the four-fermion interaction. As in the case of the Yukawa-coupling and the fermionic wave-function renormalization, we encounter additional threshold-functions in gauges with gauge-fixing parameter  $\xi \neq 1$ . We start, however, with the discussion of the threshold functions that are closely related to those already discussed in Refs. [29, 30, 100]:

$$\begin{aligned} L_{1,1,n_1,n_2}^{(FB),(d)}(\tilde{t}, \omega_\psi, \tilde{\mu}_1, \tilde{\mu}_2, \omega_{B,1}, \omega_{B,2}; \eta_\psi, \eta_B) \\ = -\frac{\tilde{t}}{2} \sum_{n=-\infty}^{\infty} \int_0^\infty dx x^{\frac{d-1}{2}} \tilde{\partial}_t \left\{ \left[ (1 + r_\psi) \tilde{G}_\psi((\tilde{\nu}_n + i\tilde{\mu}_1)^2, \omega_\psi) \right] \left[ (1 + r_\psi) \tilde{G}_\psi((\tilde{\nu}_n + i\tilde{\mu}_2)^2, \omega_\psi) \right] \times \right. \\ \left. \times \left[ \tilde{G}_B(\tilde{\nu}_n^2, \omega_{B,1}) \right]^{n_1} \left[ \tilde{G}_B(\tilde{\nu}_n^2, \omega_{B,2}) \right]^{n_2} \right\}. \quad (\text{B34}) \end{aligned}$$

By performing the integration over  $x$ , we obtain the expression for the threshold function used in this work:

$$\begin{aligned}
& L_{1,1,n_1,n_2}^{(FB),(d)}(\tilde{t}, \omega_\psi, \tilde{\mu}_1, \tilde{\mu}_2, \omega_{B,1}, \omega_{B,2}; \eta_\psi, \eta_B) \\
&= \frac{2\tilde{t}}{d-1} \sum_{n=-\infty}^{\infty} \mathcal{G}_\psi((\tilde{\nu}_n + i\tilde{\mu}_1)^2, \omega_\psi) \mathcal{G}_\psi((\tilde{\nu}_n + i\tilde{\mu}_2)^2, \omega_\psi) \left[ \mathcal{G}_B(\tilde{\nu}_n^2, \omega_{B,1}) \right]^{n_1} \left[ \mathcal{G}_B(\tilde{\nu}_n^2, \omega_{B,2}) \right]^{n_2} \times \\
&\times \left\{ \left( \mathcal{G}_\psi((\tilde{\nu}_n + i\tilde{\mu}_1)^2, \omega_\psi) + \mathcal{G}_\psi((\tilde{\nu}_n + i\tilde{\mu}_2)^2, \omega_\psi) + n_1 \mathcal{G}_B(\tilde{\nu}_n^2, \omega_{B,1}) + n_2 \mathcal{G}_B(\tilde{\nu}_n^2, \omega_{B,2}) - 1 \right) \right. \\
&\quad - \frac{\eta_B}{d+1} \left( n_1 \mathcal{G}_B(\tilde{\nu}_n^2, \omega_{B,1}) + n_2 \mathcal{G}_B(\tilde{\nu}_n^2, \omega_{B,2}) \right) \\
&\quad \left. - \frac{\eta_\psi}{d} \left( \mathcal{G}_\psi((\tilde{\nu}_n + i\tilde{\mu}_1)^2, \omega_\psi) + \mathcal{G}_\psi((\tilde{\nu}_n + i\tilde{\mu}_2)^2, \omega_\psi) - 1 \right) \right\}. \tag{B35}
\end{aligned}$$

Since we are explicitly studying Landau-gauge QCD, we have an additional class of threshold functions given by

$$\begin{aligned}
& \mathcal{L}_{1,1,n}^{(FB),(d)}(\tilde{t}, \omega_\psi, \tilde{\mu}_1, \tilde{\mu}_2, \omega_B; \eta_\psi, \eta_B) \\
&= -\frac{\tilde{t}}{2} \sum_{n=-\infty}^{\infty} \int_0^\infty dx \frac{x^{\frac{d+1}{2}}}{\tilde{\nu}^2 + x} \tilde{\partial}_t \left\{ \left[ (1+r_\psi) \tilde{G}_\psi((\tilde{\nu}_n + i\tilde{\mu}_1)^2, \omega_\psi) \right] \times \right. \\
&\quad \left. \times \left[ (1+r_\psi) \tilde{G}_\psi((\tilde{\nu}_n + i\tilde{\mu}_2)^2, \omega_\psi) \right] \left[ \tilde{G}_B(\tilde{\nu}_n^2, \omega_B) \right]^n \right\}. \tag{B36}
\end{aligned}$$

Inserting the regulator shape functions (B4), we find

$$\begin{aligned}
& \mathcal{L}_{1,1,n}^{(FB),(d)}(\tilde{t}, \omega_\psi, \tilde{\mu}_1, \tilde{\mu}_2, \omega_B; \eta_\psi, \eta_B) \\
&= \tilde{t} \sum_{n=-\infty}^{\infty} \mathcal{G}_\psi((\tilde{\nu}_n + i\tilde{\mu}_1)^2, \omega_\psi) \mathcal{G}_\psi((\tilde{\nu}_n + i\tilde{\mu}_2)^2, \omega_\psi) \left[ \mathcal{G}_B(\tilde{\nu}_n^2, \omega_B) \right]^n \times \\
&\times \left\{ H_{(d-1)}^{(1)}(\tilde{\nu}_n^2) \left( \mathcal{G}_\psi((\tilde{\nu}_n + i\tilde{\mu}_1)^2, \omega_\psi) + \mathcal{G}_\psi((\tilde{\nu}_n + i\tilde{\mu}_2)^2, \omega_\psi) + n \mathcal{G}_B(\tilde{\nu}_n^2, \omega_B) - 1 \right) \right. \\
&\quad - \frac{\eta_B}{2} \left( H_{(d-1)}^{(1)}(\tilde{\nu}_n^2) - H_{(d+1)}^{(1)}(\tilde{\nu}_n^2) \right) n \mathcal{G}_B(\tilde{\nu}_n^2, \omega_B) \\
&\quad \left. - \eta_\psi \left( H_{(d-1)}^{(1)}(\tilde{\nu}_n^2) - H_d^{(1)}(\tilde{\nu}_n^2) \right) \left( \mathcal{G}_\psi((\tilde{\nu}_n + i\tilde{\mu}_1)^2, \omega_\psi) + \mathcal{G}_\psi((\tilde{\nu}_n + i\tilde{\mu}_2)^2, \omega_\psi) - 1 \right) \right\}. \tag{B37}
\end{aligned}$$

- 
- [1] P. Braun-Munzinger, J. Stachel, and C. Wetterich, Phys. Lett. **B596**, 61 (2004), nucl-th/0311005.
- [2] P. de Forcrand and O. Philipsen, Nucl. Phys. **B642**, 290 (2002), hep-lat/0205016.

- [3] M. D’Elia and M.-P. Lombardo, Phys. Rev. **D67**, 014505 (2003), hep-lat/0209146.
- [4] P. de Forcrand and O. Philipsen, Nucl. Phys. **B673**, 170 (2003), hep-lat/0307020.
- [5] P. de Forcrand and O. Philipsen, JHEP **01**, 077 (2007), hep-lat/0607017.
- [6] Z. Fodor and S. D. Katz, Phys. Lett. **B534**, 87 (2002), hep-lat/0104001.
- [7] F. Karsch et al., Nucl. Phys. Proc. Suppl. **129**, 614 (2004), hep-lat/0309116.
- [8] Z. Fodor and S. D. Katz, JHEP **04**, 050 (2004), hep-lat/0402006.
- [9] Z. Fodor, C. Guse, S. D. Katz, and K. K. Szabo, PoS **LAT2007**, 189 (2007), arXiv:0712.2702 [hep-lat].
- [10] R. V. Gavai and S. Gupta (2008), arXiv:0806.2233 [hep-lat].
- [11] C. Schmidt, PoS **LAT2006**, 021 (2006), hep-lat/0610116.
- [12] O. Philipsen (2008), arXiv:0808.0672 [hep-ph].
- [13] Y. Nambu and G. Jona-Lasinio, Phys. Rev. **122**, 345 (1961).
- [14] M. D’Elia, A. Di Giacomo, and C. Pica, Phys. Rev. **D72**, 114510 (2005), hep-lat/0503030.
- [15] Y. Aoki, G. Endrodi, Z. Fodor, S. D. Katz, and K. K. Szabo, Nature **443**, 675 (2006), hep-lat/0611014.
- [16] J. Braun and B. Klein, Phys. Rev. **D77**, 096008 (2008), arXiv:0712.3574 [hep-th].
- [17] B. Klein and J. Braun, PoS **LAT2007**, 198 (2007), arXiv:0710.1161 [hep-lat].
- [18] J. Braun and B. Klein (2008), arXiv:0810.0857 [hep-ph].
- [19] M. A. Stephanov, PoS **LAT2006**, 024 (2006), hep-lat/0701002.
- [20] P. N. Meisinger and M. C. Ogilvie, Phys. Lett. **B379**, 163 (1996), hep-lat/9512011.
- [21] R. D. Pisarski, Phys. Rev. **D62**, 111501 (2000), hep-ph/0006205.
- [22] K. Fukushima, Phys. Lett. **B591**, 277 (2004), hep-ph/0310121.
- [23] J. Braun, K. Schwenzer, and H.-J. Pirner, Phys. Rev. **D70**, 085016 (2004), hep-ph/0312277.
- [24] E. Megias, E. Ruiz Arriola, and L. L. Salcedo, Phys. Rev. **D74**, 065005 (2006), hep-ph/0412308.
- [25] C. Ratti, M. A. Thaler, and W. Weise, Phys. Rev. **D73**, 014019 (2006), hep-ph/0506234.
- [26] C. Sasaki, B. Friman, and K. Redlich, Phys. Rev. **D75**, 074013 (2007), hep-ph/0611147.
- [27] B.-J. Schaefer, J. M. Pawłowski, and J. Wambach, Phys. Rev. **D76**, 074023 (2007), arXiv:0704.3234 [hep-ph].
- [28] B.-J. Schaefer and J. Wambach, Nucl. Phys. **A757**, 479 (2005), nucl-th/0403039.
- [29] H. Gies and C. Wetterich, Phys. Rev. **D65**, 065001 (2002), hep-th/0107221.

- [30] H. Gies and C. Wetterich, Phys. Rev. **D69**, 025001 (2004), hep-th/0209183.
- [31] J. Braun and H. Gies, Phys. Lett. **B645**, 53 (2007), hep-ph/0512085.
- [32] J. Braun and H. Gies, JHEP **06**, 024 (2006), hep-ph/0602226.
- [33] J. Braun, H. Gies, and J. M. Pawłowski (2007), arXiv:0708.2413 [hep-th].
- [34] F. Marhauser and J. M. Pawłowski, (in preparation).
- [35] J. Meyer, K. Schwenzer, H.-J. Pirner, and A. Deandrea, Phys. Lett. **B526**, 79 (2002), hep-ph/0110279.
- [36] M. Buballa, Phys. Rept. **407**, 205 (2005), hep-ph/0402234.
- [37] N. Tetradis and C. Wetterich, Nucl. Phys. **B422**, 541 (1994), hep-ph/9308214.
- [38] G. Papp, B. J. Schaefer, H. J. Pirner, and J. Wambach, Phys. Rev. **D61**, 096002 (2000), hep-ph/9909246.
- [39] B.-J. Schaefer and H.-J. Pirner, Nucl. Phys. **A660**, 439 (1999), nucl-th/9903003.
- [40] G. Von Gersdorff and C. Wetterich, Phys. Rev. **B64**, 054513 (2001), hep-th/0008114.
- [41] J. Berges, D. U. Jungnickel, and C. Wetterich, Phys. Rev. **D59**, 034010 (1999), hep-ph/9705474.
- [42] J. Berges, N. Tetradis, and C. Wetterich, Phys. Rept. **363**, 223 (2002), hep-ph/0005122.
- [43] H. Gies and J. Jaeckel, Eur. Phys. J. **C46**, 433 (2006), hep-ph/0507171.
- [44] J. M. Pawłowski, Annals Phys. **322**, 2831 (2007), hep-th/0512261.
- [45] G. 't Hooft, Phys. Rev. **D14**, 3432 (1976), Erratum-ibid. **D18**:2199 (1978).
- [46] M. A. Shifman, A. I. Vainshtein, and V. I. Zakharov, Nucl. Phys. **B163**, 46 (1980).
- [47] E. V. Shuryak, Nucl. Phys. **B203**, 93 (1982).
- [48] T. Schafer and E. V. Shuryak, Rev. Mod. Phys. **70**, 323 (1998), hep-ph/9610451.
- [49] R. D. Pisarski and F. Wilczek, Phys. Rev. **D29**, 338 (1984).
- [50] C. Wetterich, Phys. Lett. **B301**, 90 (1993).
- [51] D. F. Litim and J. M. Pawłowski, JHEP **11**, 026 (2006), hep-th/0609122.
- [52] J.-P. Blaizot, A. Ipp, R. Mendez-Galain, and N. Wschebor, Nucl. Phys. **A784**, 376 (2007), hep-ph/0610004.
- [53] D. F. Litim and J. M. Pawłowski, Phys. Lett. **B516**, 197 (2001), hep-th/0107020.
- [54] D. F. Litim, Phys. Lett. **B486**, 92 (2000), hep-th/0005245.
- [55] D. F. Litim, Phys. Rev. **D64**, 105007 (2001), hep-th/0103195.
- [56] D. F. Litim and J. M. Pawłowski (1998), hep-th/9901063.

- [57] J. Polonyi, Central Eur. J. Phys. **1**, 1 (2003), hep-th/0110026.
- [58] H. Gies (2006), hep-ph/0611146.
- [59] D. F. Litim, Nucl. Phys. **B631**, 128 (2002), hep-th/0203006.
- [60] C. Bervillier, A. Juttner, and D. F. Litim, Nucl. Phys. **B783**, 213 (2007), hep-th/0701172.
- [61] D. Litim, C. Wetterich, and N. Tetradis, Mod. Phys. Lett. **A12**, 2287 (1997), hep-ph/9407267.
- [62] D. U. Jungnickel and C. Wetterich, Phys. Rev. **D53**, 5142 (1996), hep-ph/9505267.
- [63] J. Jaeckel (2003), hep-ph/0309090.
- [64] J. Jaeckel and C. Wetterich, Phys. Rev. **D68**, 025020 (2003), hep-ph/0207094.
- [65] H. Gies, Phys. Rev. **D66**, 025006 (2002), hep-th/0202207.
- [66] L. F. Abbott, Nucl. Phys. **B185**, 189 (1981).
- [67] M. Reuter and C. Wetterich, Nucl. Phys. **B417**, 181 (1994).
- [68] M. Reuter and C. Wetterich, Phys. Rev. **D56**, 7893 (1997), hep-th/9708051.
- [69] F. Freire, D. F. Litim, and J. M. Pawłowski, Phys. Lett. **B495**, 256 (2000), hep-th/0009110.
- [70] F. Freire, D. F. Litim, and J. M. Pawłowski, Int. J. Mod. Phys. **A16**, 2035 (2001), hep-th/0101108.
- [71] J. M. Pawłowski, Int. J. Mod. Phys. **A16**, 2105 (2001).
- [72] D. F. Litim and J. M. Pawłowski, JHEP **09**, 049 (2002), hep-th/0203005.
- [73] D. F. Litim and J. M. Pawłowski, Phys. Lett. **B546**, 279 (2002), hep-th/0208216.
- [74] A. Cucchieri, A. Maas, and T. Mendes, Phys. Rev. **D75**, 076003 (2007), hep-lat/0702022.
- [75] U. Ellwanger, M. Hirsch, and A. Weber, Z. Phys. **C69**, 687 (1996), hep-th/9506019.
- [76] D. F. Litim and J. M. Pawłowski, Phys. Lett. **B435**, 181 (1998), hep-th/9802064.
- [77] A. Sternbeck, E. M. Ilgenfritz, M. Müller-Preussker, A. Schiller, and I. L. Bogolubsky, PoS **LAT2006**, 076 (2006), hep-lat/0610053.
- [78] F. D. R. Bonnet, P. O. Bowman, D. B. Leinweber, and A. G. Williams, Phys. Rev. **D62**, 051501 (2000), hep-lat/0002020.
- [79] J. Gattnar, K. Langfeld, and H. Reinhardt, Phys. Rev. Lett. **93**, 061601 (2004), hep-lat/0403011.
- [80] D. Dudal, R. F. Sobreiro, S. P. Sorella, and H. Verschelde, Phys. Rev. **D72**, 014016 (2005), hep-th/0502183.
- [81] A. Cucchieri, T. Mendes, O. Oliveira, and P. J. Silva, Phys. Rev. **D76**, 114507 (2007),



0705.3367.

- [82] L. von Smekal, R. Alkofer, and A. Hauck, Phys. Rev. Lett. **79**, 3591 (1997), hep-ph/9705242.
- [83] L. von Smekal, A. Hauck, and R. Alkofer, Ann. Phys. **267**, 1 (1998), hep-ph/9707327.
- [84] C. S. Fischer, R. Alkofer, and H. Reinhardt, Phys. Rev. **D65**, 094008 (2002), hep-ph/0202195.
- [85] C. S. Fischer and R. Alkofer, Phys. Lett. **B536**, 177 (2002), hep-ph/0202202.
- [86] J. M. Pawłowski, D. F. Litim, S. Nedelko, and L. von Smekal, Phys. Rev. Lett. **93**, 152002 (2004), hep-th/0312324.
- [87] C. S. Fischer and H. Gies, JHEP **10**, 048 (2004), hep-ph/0408089.
- [88] S. Mandelstam, Phys. Rev. **D20**, 3223 (1979).
- [89] D. Zwanziger, Phys. Rev. **D65**, 094039 (2002), hep-th/0109224.
- [90] C. Lerche and L. von Smekal, Phys. Rev. **D65**, 125006 (2002), hep-ph/0202194.
- [91] C. S. Fischer and J. M. Pawłowski, Phys. Rev. **D75**, 025012 (2007), hep-th/0609009.
- [92] S. Bethke, Nucl. Phys. Proc. Suppl. **135**, 345 (2004), hep-ex/0407021.
- [93] C. S. Fischer, A. Maas, and J. M. Pawłowski (2008), 0810.1987.
- [94] J. Braun, (in preparation).
- [95] D. Toublan, Phys. Lett. **B621**, 145 (2005), hep-th/0501069.
- [96] J. M. Pawłowski, Phys. Rev. **D58**, 045011 (1998), hep-th/9605037.
- [97] J. Braun and J. M. Pawłowski, (in preparation).
- [98] G. I. S. and R. I. M., *Table of integrals, series, and products* (2000), 6th ed., Jeffrey, Alan (ed.), Academic Press, San Diego (2000).
- [99] F. Hofling, C. Nowak, and C. Wetterich, Phys. Rev. **B66**, 205111 (2002), cond-mat/0203588.
- [100] E. Meggiolaro and C. Wetterich, Nucl. Phys. **B606**, 337 (2001), hep-ph/0012081.